RL-TR-91-95
Final Technical Report
July 1991

ON THE ROLE OF CRYSTAL DEFECTS AS SOURCES OF RESONATOR FREQUENCY INSTABILITY

Columbia University

A.S. Nowick

APPROVED FOR PUBLIC RELEASE; DISTRIBUTION UNLIMITED.

Rome Laboratory
Air Force Systems Command
Griffiss Air Force Base, NY 13441-5700

This report has been reviewed by the Rome Laboratory Public Affairs Division (PA) and is releasable to the National Technical Information Service (NTIS). At NTIS it will be releasable to the general public, including foreign nations.

RL-TR-91-95 has been reviewed and is approved for publication.

APPROVED: Herbert G. Lipson

HERBERT G. LIPSON
Project Engineer

APPROVED: Harold Roth

HAROLD ROTH
Director of Solid State Sciences

FOR THE COMMANDER: James W. Hyde III

JAMES W. HYDE III
Directorate of Plans & Programs

If your address has changed or if you wish to be removed from the Rome Laboratory mailing list, or if the addressee is no longer employed by your organization, please notify Rome Laboratory (ESE) Hanscom AFB MA 01731-5000. This will assist us in maintaining a current mailing list.

Do not return copies of this report unless contractual obligations or notices on a specific document require that it be returned.

REPORT DOCUMENTATION PAGE

Form Approved
OMB No. 0704-0188

1. AGENCY USE ONLY (Leave Blank)	2. REPORT DATE	3. REPORT TYPE AND DATES COVERED
	July 1991	Final Jun 85 - Aug 88

4. TITLE AND SUBTITLE
ON THE ROLE OF CRYSTAL DEFECTS AS SOURCES OF RESONATOR FREQUENCY INSTABILITY

5. FUNDING NUMBERS
C - F19628-85-C-0104
PE - 61102F
PR - 2305
TA - J1
WU - 46

6. AUTHOR(S)
A. S. Nowick

7. PERFORMING ORGANIZATION NAME(S) AND ADDRESS(ES)
Henry Krumb School of Mines
Columbia University
New York NY 10027

8. PERFORMING ORGANIZATION REPORT NUMBER
N/A

9. SPONSORING/MONITORING AGENCY NAME(S) AND ADDRESS(ES)
Rome Laboratory (ESE)
Hanscom AFB MA 01731-5000

10. SPONSORING/MONITORING AGENCY REPORT NUMBER
RL-TR-91-95

11. SUPPLEMENTARY NOTES
Rome Laboratory Project Engineer: Herbert G. Lipson/ESE/(617) 377-3297

12a. DISTRIBUTION/AVAILABILITY STATEMENT
Approved for public release; distribution unlimited.

12b. DISTRIBUTION CODE

13. ABSTRACT (Maximum 200 words)

This work involved the study of defects in quartz crystals, primarily by the use of electrical measurements, viz. electrical conductivity and dielectric relaxation (DR) measurements. The latter has turned out to be a powerful tool since it is capable of detecting dipolar defects that other techniques, e.g. electron paramagnetic resonance (EPR) and infrared absorption (IR), cannot detect, as well as defects that EPR can also measure. DR peaks have been observed that are produced by Al-Na defects in two different configurations, by Al-hole defects, and by several types of defects involving Fe, in the case of Fe-containing crystals. In all cases, we have worked to identify the responsible defect, to correlate it with defects measured by EPR and IR techniques, and to determine the interactions of the defect with the lattice. Special attention has also been given to the role of ionizing radiation (X-ray and γ-rays) and of subsequent annealing on these various defects. The role of irradiation is of special importance when quartz crystals are used in hostile environments.

14. SUBJECT TERMS	15. NUMBER OF PAGES
Quarts, Defect Structure of Solids, Electrical Properties, Dielectric Properties	44
	16. PRICE CODE

17. SECURITY CLASSIFICATION OF REPORT	18. SECURITY CLASSIFICATION OF THIS PAGE	19. SECURITY CLASSIFICATION OF ABSTRACT	20. LIMITATION OF ABSTRACT
UNCLASSIFIED	UNCLASSIFIED	UNCLASSIFIED	UL

DISCLAIMER NOTICE

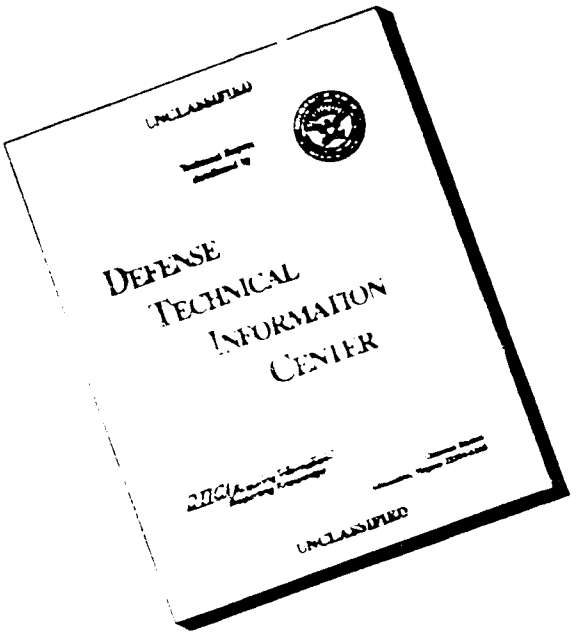

THIS DOCUMENT IS BEST QUALITY AVAILABLE. THE COPY FURNISHED TO DTIC CONTAINED A SIGNIFICANT NUMBER OF PAGES WHICH DO NOT REPRODUCE LEGIBLY.

40th Annual Frequency Control Symposium - 1986

STUDY OF IRRADIATION EFFECTS IN QUARTZ CRYSTALS USING LOW-TEMPERATURE DIELECTRIC RELAXATION

S. Ling and A. S. Nowick
Henry Krumb School of Mines, Columbia University
New York, NY 10027.

Summary

A study is made of irradiation effects on α-quartz crystals using the technique of dielectric loss measurements at low temperatures. Sodium-swept quartz shows a pair of loss peaks (at 30 K and 75 K for a 1 kHz frequency) that are due to the Al-Na defect. These peaks generally decrease after irradiation and a new "irradiation peak" appears in the range of 8 to 12 K. The fact that this "irradiation peak" also appears in a vacuum swept sample and in the same proportion as Al-hole centers strongly shows that this peak is related to the Al-hole center. Measurements of the two Al-Na peaks and the irradiation peak permits us to follow defect changes in quartz as a result of X-ray irradiation and subsequent annealing. Restoration of the main Al-Na peak during annealing occurs in two stages: one near 500 K and the other above 600 K. A defect model interpreting these two stages is presented.

Introduction

The relation of lattice defects to frequency instabilities of quartz crystal resonators, both before and after irradiation, has been much discussed in these Symposia[1] and elsewhere.[2,3] The purpose of the present paper is to show that dielectric loss measurements at cryogenic temperatures constitutes an important tool for the study of defects in quartz. Especially when used in combination with other techniques, such as infrared (IR) absorption, electron spin resonance (ESR) and anelastic relaxation, it is able to give considerable information about the defect structure of quartz crystals.

The principal defects present in as-grown cultured quartz crystals center about Al^{3+} impurities substituting for Si^{4+}. Because of the charge difference, Al^{3+} ions must be compensated by monovalent ions, e.g. Li^+, Na^+ or H^+, located in interstitial sites adjacent to the substitutional Al. The Al-Na pair manifests itself strikingly through two dielectric loss peaks at 30 K and 75 K (for a frequency of 1 kHz) known as the α and β peaks, respectively.[4,5] This defect also produces an analogous pair of mechanical loss, or anelastic relaxation, peaks.[6,7] It is known that the α and β defects involve the Na^+ located on opposite sides of the distorted AlO_4 tetrahedron.[5,8] Since the Na interstitial site is located off the two-fold (C_2) symmetry axis (the x-axis), there are two equivalent α sites and two equivalent β sites on any one tetrahedron, as shown in Fig. 1. The dielectric and anelastic relaxation processes are due to the reorientation of the Na^+ between either pair of equivalent sites. Since the α site is more highly occupied than the β, it is reasonable to expect that there is a free energy difference, Δg (>0) such that, under equilibrium conditions at temperature T, the occupation ratio will be given by:

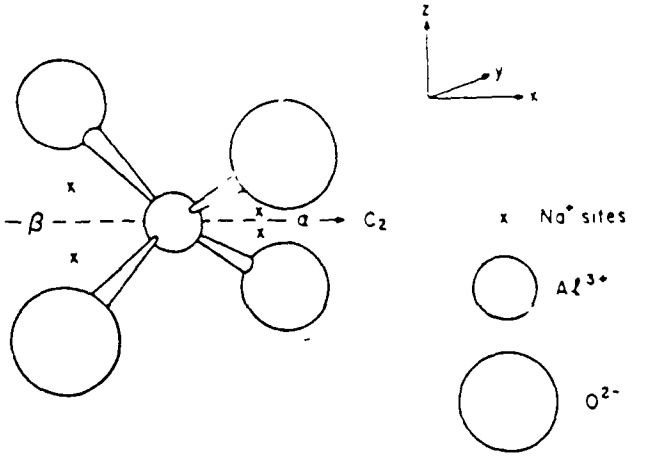

Fig. 1. Schematic diagram showing the distorted tetrahedron, the basic structural unit of α-quartz, with Al^{3+} replacing Si^{4+}. The tetrahedron contains a single twofold symmetry axis (in the x direction) designated C_2. Also shown are the two equivalent α-sites and the two equivalent β-sites. An interstitial Na^+ compensating the Al^{3+} will go into one of these four sites.

$$N_\alpha/N_\beta = \exp(\Delta g/kT) \qquad (1)$$

In the case of Li^+ compensation, an Al-Li pair is formed, but in this case the Li^+ sits on the C_2 axis; accordingly no dielectric or anelastic relaxation is observed.[7,8] Since Li^+ is present in the mineralizer during growth of most cultured crystals, the Al-Li defect tends to predominate. However Li^+ can be exchanged for Na^+ by electrodiffusion or "sweeping" with a Na salt at the anode.[6,7] In such a Na-swept sample most Al is in the form of Al-Na pairs. The alkalis can also be replaced by H^+ through sweeping in moist air, to produce Al-OH centers.

The remaining important defects in quartz are the "grown-in OH centers" which manifest themselves through IR absorption bands near 3500 cm^{-1}.[9-11] These centers are different from Al-OH, but the nature of these defect centers have not yet been established.

Irradiation of quartz crystals with high-energy photons (X-rays or γ-rays) produces large numbers of electron-hole pairs. When irradiation is carried out above 200 K, it gives rise to changes in the defects, such that alkalis originally paired with Al are replaced by H^+ (as Al-OH centers) or holes (to form Al-h centers). (The former are detected by IR and the

latter by ESR.[12,13]) In addition, upon irradiation a dielectric relaxation peak is also observed near 10 K. Originally this peak was attributed to Al-h centers[14] but later results suggested that perhaps it might be due to an alkali center.[15] To keep open its origin, we simply refer to it as the "irradiation peak". In the present work we follow the production of this peak by irradiation and its disappearance during annealing. At the same time, by using Na-swept samples, we can follow the concurrent changes in the α and β peaks. In this way, we hope to learn more about defect processes that take place during irradiation and annealing.

In addition, since Al-h centers have been found in vacuum-swept samples without irradiation[16], we wished to examine such samples to see if the "irradiation peak" is also present under these conditions. In this way, we have an opportunity to establish the identity of the irradiation peak.

Theory

A defect that has lower point symmetry than its host crystal has several crystallographically equivalent orientations, among which it can reorient preferentially in the presence of an electric field.[17] If a sinusoidal electric field with angular frequency ω is applied to the system, the reorientation of the defect among its equivalent orientations give can give rise to one or more peaks in dielectric loss, tan δ, which obey the Debye equation:

$$\tan \delta = \varepsilon''/\varepsilon' = (\delta\varepsilon/\varepsilon_\infty).(\omega\tau/1+\omega^2\tau^2) \qquad (2)$$

where ε", ε' are the imaginary and real parts of the complex dielectric constant, ε_∞ the high frequency dielectric constant, δε the relaxation of the dielectric constant, and τ the relaxation time, often given by:

$$\tau^{-1} = \nu_o.\exp(-E/kT) \qquad (3)$$

Here E is the activation enthalpy, kT its usual meaning, and ν_o the pre-exponential factor. For a field parallel to the z-direction (the c-axis), the maximum peak height is given by:

$$\tan \delta_{max} = \delta\varepsilon/2\varepsilon_\infty = N_d\mu_3^2/2\varepsilon_o kT \qquad (4)$$

where N_d is the concentration of the defect (in number/volume), μ_3 is the component of the defect dipole moment in the z-direction, and ε_o is the permittivity of free space.

For the Al-Na defect in quartz crystal, as already mentioned, two Debye peaks denoted as the α and β peaks are observed. A useful and measurable quantity, the ratio of the α to β peak heights, can be deduced from equation (4) to be:

$$R = \tan \delta_{max}^{\alpha}/\tan \delta_{max}^{\beta} = (N_\alpha/N_\beta).(T_\beta/T_\alpha).(\mu_3^\alpha/\mu_3^\beta)^2 \qquad (5)$$

where T_α and T_β are the two peak temperatures, and μ_3^α and μ_3^β are the respective z-component of the dipole moments. Previous work showed that $T_\beta/T_\alpha = 75/30$ while $\mu_3^\alpha/\mu_3^\beta = 0.5(\pm 0.1)$.[8] Thus, from the ratio R, we can obtain N_α/N_β, but in absolute accuracy only to within ± 40%.

Table I. Crystals used in this work.

Designation	Source	Al content (ppma)
PQE	Sawyer Co. (U.S.)	17
QA26	U.S. Air Force RADC	55
H29-14	U.S. Air Force RADC	4
NQ	Natural (U.S.)	53

Experimental Details

Crystals Used

Various cultured and a natural crystals were used in this study. The different crystals used, with their designations and sources, are listed in Table I. The Al contents, given in the last column, were obtained from the heights of the Al-Na dielectric loss peak heights[8], except that for the vacuum swept H29-14 which was obtained from ESR measurement made by Halliburton at Okalahoma State University.[16] Na^+-sweeping of the crystals were carried out at Okalahoma State by Martin, and vacuum sweeping was carried out at RADC, Hanscom AFB.

All samples were cut with cross section of approximately 1.0 x 1.0 cm^2 and thickness of approximately 1 mm, the latter dimension being parallel to the c-axis.

Irradiation and Measurement

Samples were irradiated at room temperature with X-rays from a tungsten target source operated at 20 mA and 40 kV. Soft X-rays were filtered out by a layer of sputtered silver electrode, and a glass filter approximately 1 mm thick. In addition, the NQ sample was also irradiated at room temperature with Y-ray from a Co source at Brookhaven National Laboratory, which has a dose rate of 1.1 MRoentgen/hr.

After irradiation, the samples were transferred to a Super Varitemp Cryostat (Janis Corp.), and cooled down to liquid helium temperature. An automated capacitance bridge (C. Andeen Assoc.) was used to carry out the dielectric loss measurements, which cover a frequency range of 30 to 100 kHz and a temperature range of 3 - 273 K.

Results and Discussion

Vacuum Swept Quartz Crystal

We would first like to address the question of the origin of the low temperature irradiation peak. As pointed out in the Introduction section, two different irradiation related defect centers have been suggested as the possible sources of this irradiation peak: (1) the Al-h center formed during irradiation, and (2) an alkali center that involves the Na^+ ion released from Al-Na during irradiation. In order to investigate these possibilities, we have made several measurements on the vacuum swept crystal, H29-14 (see Table I). The crystal was first swept in air, and then in vacuum for an extended period of time to ensure that all alkali and hydrogen ions have been swept out.

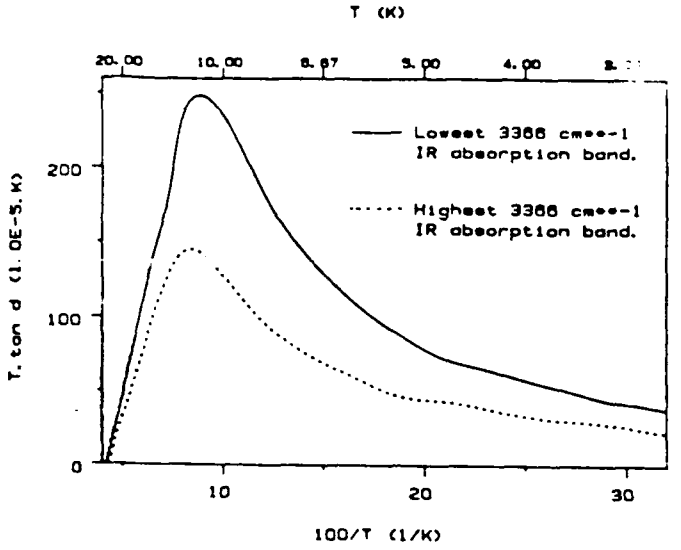

Fig. 2. Dielectric loss peaks, plotted as T.tan δ vs. 1/T, for two vacuum-swept H29-14 samples with different 3366 cm^{-1} IR absorption: solid line, α_x = 0.025 cm^{-1}, and dashed line, α_x = 0.3 - 0.4 cm^{-1}.

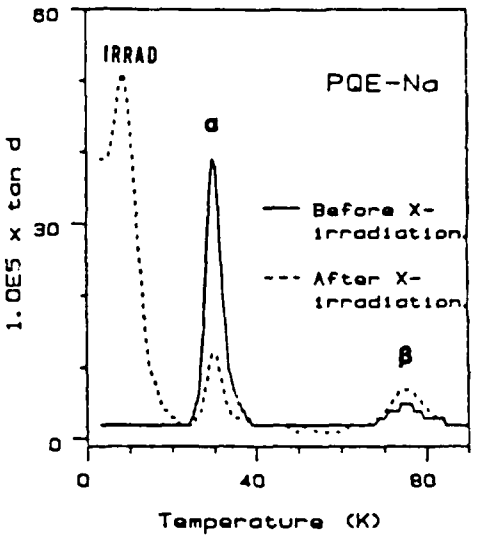

Fig. 3. Dielectric loss as a function of temperature before and after irradiation for a Na-swept PQE crystal as measured at 1 kHz. The data show the Al-Na α and β peaks as well as the irradiation peak.

The IR absorption spectrum of this vacuum-swept crystal measured by Lipson at RADC showed that the crystal is not uniformly swept. While the crystal has no 3581 cm^{-1} absorption (corresponding to grown-in OH) throughout, it showed varying degree of 3366 cm^{-1} absorption (corresponding to Al-OH) along the z-direction, i.e. along the c-axis. We studied two samples by means of dielectric measurements: one from the best swept region which has the lowest 3366 cm^{-1} absorption (α_x ~ 0.025 cm^{-1}), and one from the worst swept region which has higher 3366 cm^{-1} absorption (α_x ~ 0.3-0.4 cm^{-1}). The results of the measurements are shown in Fig. 2 as plots of T.tanδ vs. 100/T. Despite the absence of alkali and the low level of hydrogen, both samples show a low temperature peak with maxima at 100/T ~ 8.5 K^{-1}. The height in the best swept sample is about twice that in the worst swept one, and their shapes are identical within experimental error. No observable change of the peaks occurs after a 321 C annealing of both samples.

It is interesting to compare the results of our dielectric measurements to the Al-h contents measured with ESR by Halliburton on samples prepared from the same vacuum swept crystal.[16] He measured 1.3 ppm of Al-h center in the best swept region, and 0.5 ppm in the worst swept region. The 2.6 : 1 ratio of the Al-h contents observed in this way correlates reasonably well with the 1.8 : 1 ratio of the dielectric peak heights that we observed in corresponding samples.

From the fact that both the "irradiation peak" and the Al-h center appear in these unirradiated vacuum-swept samples despite the absence of alkali, we conclude that the irradiation peak cannot be due to the alkali center, but that it must be some manifestation of the Al-h center.

Effect of Irradiation Dose

In order to investigate the effect of irradiation dose on defects in quartz crystals, we have carried out a series of room temperature X-ray irradiations on a Na-swept PQE crystal, and measured the corresponding changes in the α and β Al-Na peaks as well as the irradiation peak. The various peaks are shown in Fig. 3, the results of the irradiation series are presented in Fig. 4. While the α peak decreases and the irradiation peak increases monotonically with the total dose, the β peak height goes through a maximum before it drops down to zero. By taking into account both the α and β peaks, however, the overall Al-Na concentration is found to be decreasing monotonically with the accumulating dose. The ratio R of α/β goes from an initial value of ~12 before the irradiation to a constant value of 2.7 ± 1 after irradiation. Values of R ranging from 10 to 17, depending on the previous heat treatment, have been observed previously,[4,5,8] but a value as low as 2.7 has never been reported. An even lower value of R of 0.85 was observed in this labratory in a Y-irradiated, Na-swept NQ crystal.

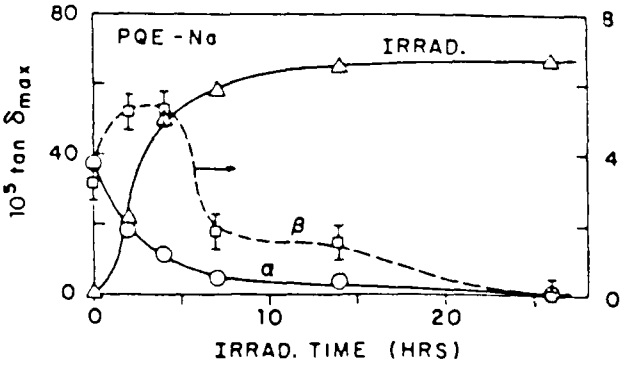

Fig. 4. Variation of the heights of the three dielectric loss peaks with X-ray irradiation time for a Na-swept PQE crystal. The left hand scale applies to the α and irradiation peaks, and the right hand scale to the β peak.

The R ratio, according to equation (5), is
>portional to the concentration ratio of the nearest
ighbor α to the next nearest neighbour β Al-Na
nters. A typical value of R = 13 before irradiation
ves N_α/N_β = 20 ± 8.5, The lower R values after
adiation correspond to smaller N_α/N_β ratios: R = 2.7
ves N_α/N_β = 4.2 ± 1.8, and the R = 0.85 mentioned
ove gives N_α/N_β = 1.4 ± 0.6. Thus it is reasonable to
that one of the effects of the irradiation is to
listribute the initial Al-Na population, which is in
ermodynamic equilibrium between the α and β states,
a more random one in which the N_α/N_β ratio comes
ch closer to unity. The maximum in the β curve shows
at initially there are more β centers formed than
stroyed, presumably at the expense of the α centers.

Based on these considerations, we propose the
llowing explanation for these observations. During
adiation, the Na^+ ion in an Al-Na center, whether α
β type, leaves the Al^{3+}, presumably through the
fluence of the electrons and holes generated by the
adiation. The Na^+ may then go to a yet unknown trap
te, or return to an Al^{3+} to reform the Al-Na center.
such a recapture, the Na^+ can go into either the α
β site. This randomizes the α/β population
stribution, giving rise to a N_α/N_β ratio closer to
ity, which results in a smaller R_β^α ratio. The maximum
the β curve is then the result of the combination of
o effects: the randomization of the N_α/N_β ratio which
uses the initial rise, and the decrease in the
erall Al-Na concentration which causes the eventual
op in the β-curve.

This dynamic picture of the irradiation induced
struction and reformation of the Al-Na centers has an
portant implication: the dissociated Al^{3+} does not
ve to capture a Na^+, but can instead capture a hole
form Al-h or a proton to form Al-OH center. The
otons are presumbly released from the grown-in OH
nters, which we called G-OH, where G designates the
unknown grown-in OH site. In other words, there
y be these three competing processes occuring during
adiation: (1) the α/β population randomization, (2)
formation of Al-h, and (3) the formation of Al-OH.
ese three reactions can be represented with the
llowing equations:

$$(\text{Al-Na})_\alpha \longleftrightarrow (\text{Al-Na})_\beta \qquad (6)$$

$$\text{Al-Na} + h^+ + e^- \longleftrightarrow \text{Al-h} + Na^\circ \qquad (7)$$

$$\text{Al-Na} + \text{G-OH} \longleftrightarrow \text{Al-OH} + \text{G-Na} \qquad (8)$$

ese processes, rather than occuring sequentially as
viously thought, are occuring simultaneously, and
competing with each other throughout the
adiation process.

ect of Annealing of an Irradiated Crystal

In order to study the annealing effects following
adiation, we utilized a Na-swept QA26 sample, which
a high Al content (see Table I). Following an
tial 4 hr irradiation at room temperature, a series
isochronal (45 min) anneals were carried out, with
ults as shown in Fig. 5. The irradiation only
ered the α peak from 120 to 90 while producing an
adiation peak of height 65 (all x10^{-5}). The
adiation peak decreases strongly between 350 and 500
nd goes to zero at 600 K, while the α peak
arently increases in two stages, the larger one at
K occuring after the irradiation peak is
pletely gone. The β peak (not shown in the figure

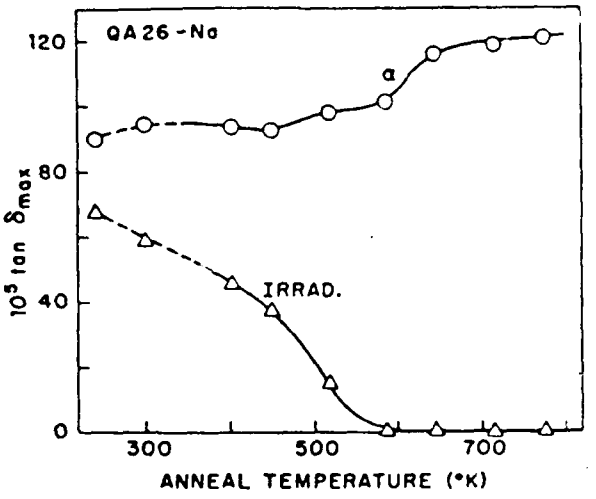

Fig. 5. Annealing of the α peak and the irradiation peak in a Na-swept QA26 crystal. The first points (shown below 300 K) were obtained immediately after irradiation; the second points (at 300 K) were measured after standing for 115 hr. All other points represent 45 min isochronal anneals.

for clarity) decreases so that the α/β ratio R returns immediately after the start of annealing to its pre-irradiated value of 13 ± 1.

It is interesting to compare these results with the annealing behavior reported by Martin, who employed IR absorption to detect Al-OH centers and acoustic loss measurements to follow both an Al-Na loss peak and an irradiation induced loss peak at 23 K (for 5 MHz frequency) believed to be due to Al-h centers.[7] The Al-Na loss peak was found to be restored in two stages that match those observed in the present work. The first stage centered at 525 K, where the 23 K loss peak disappeared, and the second centered at 650 K where Al-OH anneals out.

These observations can be explained as follow: (1) prior to the occurence of stage I, at just above room temperature, the thermodynamic equilibrium between α and β type Al-Na centers is restored. This causes the α/β ratio, R, to be restored to its pre-irradiated value. (2) Stage I annealing, which occurs between 450 and 550 K, involves the recombination and mutual annihilation of the electrons and holes, to eliminate the alkali centers and the Al-h centers, which cause the irradiation peak. This reaction is just the reverse of equation (7). (Additional support for the concept that electrons and holes become mobile in stage I comes from the fact that the E_1' center, which involves an electron trapped at an oxygen vacancy, only forms after irradiation followed by annealing at stage I temperatures.[18]) (3) Stage II annealing, which occurs between 600 and 700 K involves the re-exchange of Na^+ and H^+ to restore the G-OH and Al-Na centers, i.e., the reverse of equation (8). Thus, by stepwise reversal of each of the radiation produced reactions, eqs. (6)-(8), the crystal is finally restored to its as-grown condition.

Conclusions

We summarize in this section what has been learne: this work:

(a) Both the Al-h centers and the "irradiation peak" are observed in the vacuum-swept quartz crystal. This shows that the irradiation peak is some manifestation of the Al-h centers.

(b) During irradiation, the defect centers that give rise to the various dielectric loss peaks undergo dynamic destruction and reformation processes. Several reactions are competing with each other and occuring simultaneously, namely the Al-Na α/β population randomization, and the formation of Al-h and Al-OH centers at the expense of Al-Na centers.

(c) During annealing, the various reactions that occured during irradiation are reversed at sucessively higher temperatures:

- The thermodynamic equilibrium between α and β Al-Na centers is restored at just above room temperature.
- Above 450 K the Al-h centers are converted back to Al-Na, presumbly with electron-hole recombination, giving rise to the stage I α-peak restoration.
- Above 600 K the Al-OH centers are converted back to Al-Na giving rise to the stage II α-peak restoration.

ile this picture of various dynamic processes curing during irradiation and annealing of quartz ystals may be too simplified, and still leaves open e question of the nature of both the G-OH center and e trapping site for the alkali center, it vertheless can serve as a starting point for a more tailed understanding of irradiation process in artz.

Acknowledgement

This work was supported by the U.S. Air Force under ntract F-19628-85-C-0104 and monitored by H.G. pson, RADC Hanscom AFB.

References

1. See numerous papers in Proceedings of the Annual Symposium on Frequency Control, 1978-1985.
2. B.R. Capone, A. Kahan, R.N. Brown and J.R. Buckmelter, IEEE Trans. Nucl. Sci., NS-13, 130 (1966); NS-17 217 (1970).
3. J.C. King and H.H. Sander, Radiation Effects, 26, 203 (1975).
4. J.M. Stevels and J. Volger, Philips Res. Rep., 17, 283 (1962).
5. D.S. Park and A.S. Nowick, Physica Stat. Solidi (a) 26, 617 (1974).
6. D.B. Fraser, in Physical Acoustics (ed. W.P. Mason), Vol. 5, Chap. 2, Academic Press, N.Y., 1968.
7. J.J. Martin, J. Appl. Phys. 56, 2536 (1984).
8. J. Toulouse and A.S. Nowick, J. Phys. Chem. Solids 46, 1285 (1985).
9. A. Kats, Philips Res. Rep. 17, 133 (1962).
10. R.N. Brown and A. Kahan, J. Phys. Chem. Solids 36, 467 (1975).
11. H.G. Lipson and A. Kahan, J. Appl. Phys. 58, 963 (1985).
12. M.E. Markes and L.E. Halliburton, J. Appl. Phys. 50, 8172 (1979).
13. L.E. Halliburton, N. Koumvakalis, M.E. Markes and J.J. Martin, J. Appl. Phys. 52, 3565 (1981).
14. W.J. de Vos and J. Volger, Physica 34, 272 (1967); 47, 13 (1970).
15. J. Toulouse and A.S. Nowick, in Proceeding of the Materials Research Society Symposium, Vol.24, p. 149 (ed. J.H. Crawford, Y. Chen and W.A. Sibley), Elsevier, N.Y., 1984.
16. L.E. Halliburton, private communication.
17. A.S. Nowick and W.R. Heller, Adv. Phys. 14, 101 (1965); 16, 1 (1967).
18. M.G. Jani, R.B.Bossoli, and L.E. Halliburton, Phys. Rev. 27, 2285 (1983).

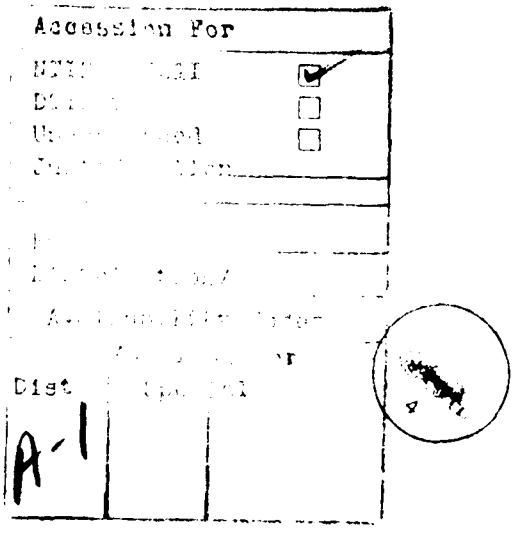

Materials Research Symposium,

Vol.60 - 1986

EFFECTS OF IRRADIATION ON THE ELECTRICAL PROPERTIES OF α-QUARTZ CRYSTALS

S. LING, B.S. LIM AND A.S. NOWICK
Henry Krumb School of Mines, Columbia University, New York NY 10027

ABSTRACT

A study is made of irradiation effects on α-quartz crystals using the techniques of electrical conductivity and dielectric loss measurements. The initial radiation-induced conductivity (RIC) induced by X-ray irradiation over the temperature range from 94 to 250 K is found to have a nearly constant activation energy of 0.29 ± 0.02 eV. Since a large RIC still results from irradiation at temperatures too low for alkalis to be liberated, it is proposed that the RIC is due to holes (as small polarons) rather than to alkalis. The dielectric loss measurements in Na-swept quartz are used to follow the changes in the relaxation peaks due to the Al-Na defect as a function of radiation dose and annealing. At the same time a low-temperature "irradiation peak" is studied. Restoration of the main Al-Na peak during annealing occurs in two stages: one near 500 K and the other above 600 K. From the observed behavior of the irradiation peak in various crystals, it is concluded that this peak is probably due to alkali centers. Finally, a defect model interpreting the two annealing stages is presented.

INTRODUCTION

The effects of particle or electromagnetic radiation on quartz crystals have been studied for many years. The subject is of interest from a practical viewpoint because irradiation gives rise to undesirable frequency changes in piezoelectric resonators made from such crystals.[1,2] From a basic viewpoint, on the other hand, irradiation produces various interesting defect centers, often involving electrons and holes, which can be studied by techniques such as optical and infrared absorption, EPR and dielectric relaxation. Such defects have been shown to be responsible for the frequency changes already mentioned.

In order to comprehend better the defects present after irradiation, we begin by reviewing the defects present in unirradiated ("as grown") crystals. The most ubiquitous and best understood defects are those involving Al^{3+} impurity ions substituting for Si^{4+} at the center of a distorted AlO_4 tetrahedron.[3] Such lower-valent impurity ions are charge compensated by either alkalis (Na^+ or Li^+) or by H^+. The alkalis, denoted M^+, are normally present in synthetically grown crystals and located adjacent to the Al^{3+} to form an Al-M pair. One alkali species can be replaced by another by a process of electrodiffusion or "sweeping" during which an appropriate salt is present at the cathode.[4,5] Alkalis can also be replaced by H^+ by sweeping in moist air, thus forming Al-OH centers that manifest themselves through two characteristic infrared absorption bands.[6] Other defects involving OH^- ions in the as-grown crystals are indicated by other IR bands, all in the vicinity of 3500 cm^{-1}.[5,6,7]

Upon irradiation near room temperature, the alkalis are liberated , and the Al-M defects become converted to both Al-OH and Al-h (aluminum-hole) centers. The fate of the liberated M^+ ions, i.e. the centers that they form after irradiation, is essentially unknown.

Electrical measurements have been very useful in the study of defects in quartz both before and after irradiation. These measurements are of two types. First, there are conductivity measurements. The conductivity of the unirradiated crystal is ionic, the carrier being mainly alkali freed

Mat. Res. Soc. Symp. Proc. Vol. 60 © 1986 Materials Research Society

Table I. Crystals Used in This Work

Designation	Source	ppm Al
SQA	Toyo Co. (Japan)	13
PQE	Sawyer Co.(U.S.)	17
QA26	U.S. Air Force RADC	55
NQ	Natural (U.S.)	53

thermally from Al-H pairs.[8] Such conductivity is usually measurable with a sensitive ac bridge at temperatures above ~400 K. After irradiation, however, a radiation-induced conductivity (RIC) is observed at much lower temperatures. It has been suggested that the large increase in conductivity represented by the RIC is due to the large increase in ionic carriers freed by the irradiation.[9,10] However, evidence opposed to this idea and suggesting that the carriers may be electron holes has recently been reported.[11]

The second type of electrical measurement is dielectric relaxation: the measurement of the dielectric loss tangent under an ac applied field at low temperatures. In unirradiated crystals two Debye-type relaxation peaks are obtained (at 30 K and 75 K respectively, for a frequency of 1 kHz) that are due to Al-Na pairs.[12,13] The two peaks, called α and β, are, respectively, due to the relaxation of nn and nnn Al-Na pairs. Usually the α peak is ~15 times larger than the β. The Na-Li pair, on the other hand, does not give rise to such peaks, presumably because Li^+ sits on the two-fold symmetry axis of the Al-OH tetrahedron while Na^+ is off-axis.[14] Upon irradiation a prominent new peak appears at temperatures ~ 8 K. This peak was studied in some detail by Volger[15] and attributed to the Al-h center. For the present, we will refer to it as the "irradiation peak."

The present work involves a more detailed study of these two types of electrical measurements in X-irradiated quartz crystals. The primary objectives are to identify the defects responsible for the RIC and for the irradiation peak. In addition, we wish to study the effects of irradiation dose and of subsequent annealing on the various dielectric loss peaks. In order to utilize the two Al-Na peaks, most of the dielectric studies were carried out on Na-swept crystals, in which virtually all of the Al is initially in the form of Al-Na pairs.

EXPERIMENTAL METHODS

A natural and various synthetic crystals were used in this study. The different crystals used, with their designations and sources, are listed in Table I. The Al content, given in the last column, was obtained from the Al-Na dielectric relaxation peak heights.[14]

Electrodiffusion experiments were carried out at Oklahoma State University by Dr. J. Martin. This included Li^+, Na^+, and H^+ sweeping respectively. Samples obtained from synthetic crystals were taken from the Z-growth regions. All samples were cut with cross section of approximately 1.0 x 1.0 cm^2 and thickness approximately 1 mm. Unless otherwise mentioned, samples were cut so that the electric field is applied parallel to the c-axis.

Samples were irradiated with X-rays from a tungsten target source operated at 20 mA and 40 kV. Soft X-rays were filtered out by a layer of sputtered silver electrode, and glass of approximately 1 mm thick. For conductivity measurements, a special cell was built such that the irradiation and measurement could be carried out below room temperature without warming up.[11] For dielectric relaxation measurements, the samples were irradiated at room temperature, transferred to a Super Varitemp cryostat (Janis Corp.), and cooled down to liquid helium temperature. Both conductivity and dielectric

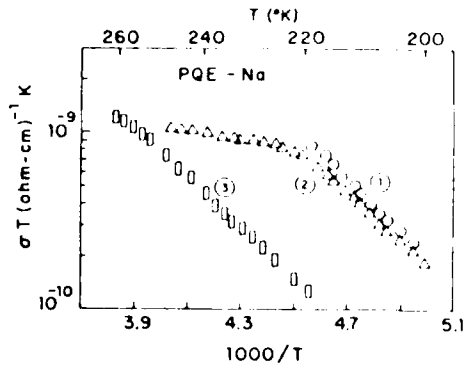

Fig. 1. (illegible) (1) (illegible) after irradiation at 294 K, (2) after anneal at 293 K, and (3) after anneal at 303 K.

relaxation measurements were made in a frequency range from 1 Hz to 1 kHz using an automated capacitance bridge (G. Andeen Assoc.).

RESULTS AND DISCUSSION

Radiation-Induced Conductivity (RIC)

Several samples were X-ray irradiated at temperatures varying from 77 to 303 K. Conductivity measurements were then made to study the evolution of the conductivity with increasing temperature, starting from the irradiation temperature. The true conductivity was separated from other effects by analyzing the frequency dependence of the conductivity.

The measured conductivity following irradiation was typically 10^{11} times that extrapolated from higher temperature measurements on the unirradiated sample, a truly spectacular result. As the temperature was increased, irreversible annealing took place, as shown in Fig. 1 for the sample PQE sample irradiated at 203 K. The results show that the conductivity level fell by about an order of magnitude in a region of annealing at 250 K. Figure 2 shows some examples of the RIC on initial warm-up after irradiation, but before appreciable annealing could occur. On the one hand, it compares the RIC for sample PQE-Na at two different irradiation temperatures, 203 and 294 K. Secondly, it shows the RIC of a H-swept SQA sample after irradiation at 94 K. The important results are that the RIC after 77 K irradiation is greater than that after 202 K irradiation for the Na-swept sample, and that no appreciable RIC is obtained from low-temperature irradiation of the H-swept sample.

Table II gives the principal results of these measurements after irradiation, reporting the activation energy E and the pre-exponential A in the Arrhenius relation for the conductivity, σ:

$$\sigma T = A \exp(-E/kT) \qquad (1)$$

It is noteworthy that E consistently falls in the range (illegible) for these and a large number of other measurements, implying the presence of a simple charge carrier. The key question is what is the identity of this charge carrier that dominates the RIC?

In earlier work, it was (illegible)

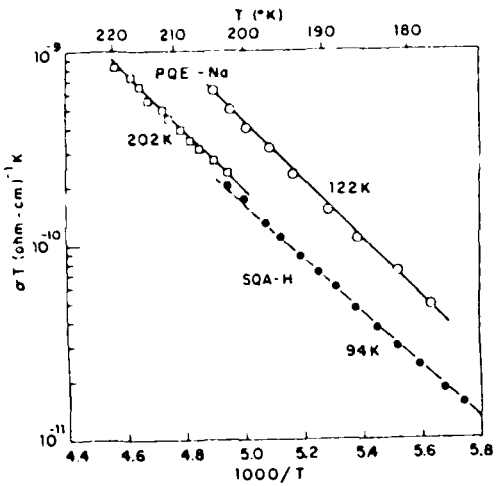

Fig. 2. RIC as a function of temperature immediately following irradiation, for Na -swept PQE and H-swept SQA samples. Irradiation temperature is marked on the curves.

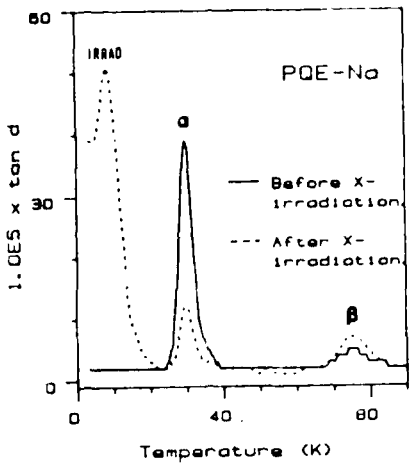

Fig. 3. Dielectric loss as a function of temperature before and after irradiation for a Na-swept PQE sample as measured at 1 kHz. The data show the Al-Na α and β peaks as well as the peak created by irradiation.

conductivity that occurs in ~ msec (after pulsed irradition) is due to electronic defects, while the longer term RIC was due to alkalis liberated from Al-M pairs.[9,10] This viewpoint was brought to question by Green et al.[11] In the light of work by Halliburton et al.[16,3] showing that alkalis were only liberated from Al-M pairs during irradiation above 200 K, Green et al. predicted that irradiation below 200 K should not give rise to a significant RIC. Nevertheless, they observed that irradiation at 150 K produced an RIC that is comparable to that from irradiation above 200 K. One might argue, however, that Halliburton used particle irradiation involving a much higher dose rate than the present X-ray irradiation; it is therefore possible that the temperature of release of alkalis may be shifted downward in the present case. Accordingly, the present experiments were designed to go much lower in irradiation temperature (see Fig.2); nevertheless, there is still no sign of a drastic decrease in RIC. In addition, the present observation of a comparable RIC in the H-swept SQA sample (Fig.2) is very significant. This sample showed a decrease in conductivity in the unirradiated state by ~ 100× as a consequence of the near elimination of alkalis by sweeping.[11] Yet Fig.2 shows that its RIC is comparable to that of crystals containing alkali. Finally, evidence by Green et al. from the annealing behavior of the RIC above room temperature is also difficult to explain in terms of alkalis as carriers.[11]

Another possibility is that the carriers are protons released by the radiation. However, there is no evidence that protons in oxides, which form strong OH⁻ bonds, have high mobility. Further, the fact that the H-swept sample shows an RIC no larger than the alkali-swept samples (Fig.2) is evidence to the contrary. Instead, it is reasonable to suggest that the carrier that dominates the RIC and migrates with an activation energy of 0.29 eV is the electron hole which behaves as a small polaron. This suggestion is not unreasonable from a theoretical viewpoint.[17] It is further supported by experiments on ultraviolet photoelectron spectroscopy in amorphous SiO_2[18]

Table II. Parameters of Initial RIC

Sample	Irrad. Temp. (K)	E (eV)	A $(\Omega\text{-cm})^{-1}$K
PQE-Na	122	0.30	1.5×10^{-2}
	202	0.28	2.3×10^{-3}
SQA-H	94	0.29	3.4×10^{-3}

Dielectric Relaxation Measurements

When a Na-swept sample is irradiated at room temperature, the two peaks (α and β) due to the Al-Na defect are substantially changed (the α peak almost decreasing) and a new "irradiation peak" develops near 8 K. Figure 3 shows these changes for the PQE-Na sample after a 4 h X ray irradiation. Here the peak has decreased from 40 to 10 as a result of the irradiation, while an irradiation peak of height 50 is created (all in tan δ units of 10^{-5}).

In order to investigate the effect of radiation dose, we have carried out a series of irradiations on the PQE-Na sample while following the changes in the α, the β and the irradiation peaks. The results are presented in Fig.4. They show that, while the α peak decreases and the irradiation peak increases monotonically with total dose, the β peak height goes through a maximum. As a result, the α/β ratio goes from an initial value of 12 before irradiation to values of 3 ± 1 after irradiation. Since this ratio measures the ratio of pp to nnn Al-Na pairs, this result means that the presence of irradiation shifts the nn ⇌ nnn equilibrium so as to correspond to a very high effective ordering temperature. In unirradiated samples, α/β ratios ranging from 10 to 17 have been observed, depending on the effective quenching-in temperature,[14] but values as low as 3 have never been seen.

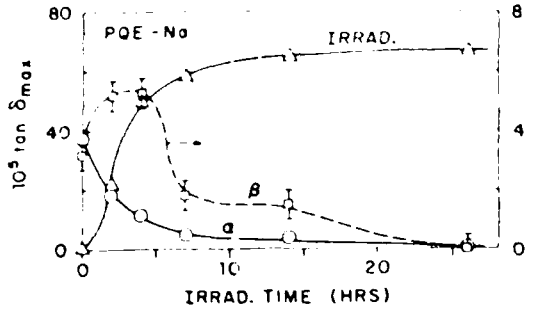

Fig. 4. Variation of the height of the [illegible] peaks with X-ray irradiation time for a Na-swept PQE sample. The left hand scale applies to the α and irradiation peaks, and the right hand scale to the β peak.

We now turn to the question of annealing effects following irradiation. For these experiments we utilized a Na-swept QA26 sample, which had a high Al content (see Table I). Following an initial 4 h irradiation at room temperature, a series of isochronal (45 min) anneals were carried out, with results as given in Fig.5. The irradiation only lowered the α peak from 120 to 90 while producing an irradiation peak of height 65 (all x 10^{-5}). The irradiation peak decreased strongly between 350 and 500 K and went to zero at 6.2 K, while the α peak apparently increased in two stages, the larger one at ~ 650 K occurring after the irradiation peak was completely gone. The β peak, not shown in Fig.5 for clarity, varied so that the α/β ratio returned to a value of 13 ± 1 immediately after the start of annealing.

It is interesting to compare these results with the annealing behavior reported by Martin [19] who employed IR absorption to detect Al-OH centers and acoustic loss measurements to follow both an Al-Na loss peak and an irradiation induced loss peak at 23 K (for 5 MHz frequency). Two annealing stages were also reported by Martin, one centered at 525 K, where the 23 K loss peak disappeared, and a second centered at 650 K where Al-OH anneals out. The Al-Na loss peak was also restored in two steps, as in the present work. It seems apparent that Martin's 23 K acoustic irradiation peak and our 8 K

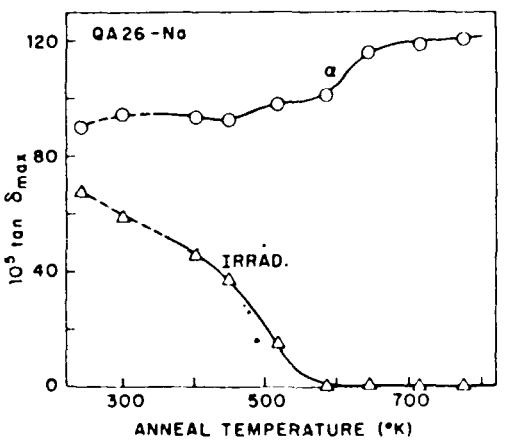

Fig. 5. Annealing of the α peak and the irradiation peak in a Na-swept QA26 sample. The first points (shown below 350 K) were obtained immediately after irradiation; the second point (at 300 K) was measured after standing for 115 h. All other points represent 45 min isochronal anneals.

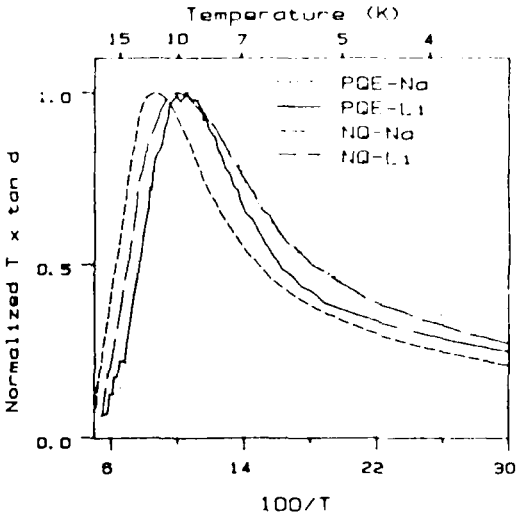

Fig. 6. Comparison of the normalized irradiation peaks for four samples: a natural crystal NQ, both Na- and Li-swept, and a synthetic crystal PQE, both Na- and Li-swept.

dielectric peak are closely related; however, Martin attributed the 23 K peak to the Al-h center, which there is now reason to doubt.[20]

A most important question is that of the origin of the present "irradiation peak". If this peak were due to the Al-h center, as had been postulated earlier,[15] it should appear unchanged in all crystals, just as the Al-h ESR spectrum is always exactly the same.[21] Instead, we find striking differences among different samples, as shown in Fig.6. This figure compares the normalized irradiation peaks (T tan δ vs. 1/T) for a natural crystal NQ, both Na- and Li-swept, and for the synthetic PQE, both Na- and Li-swept. It is clear that the peaks for the NQ crystal fall at substantially higher temperatures than those of the PQE and also that there is a 2 K shift between NQ-Na and NQ-Li, with the NQ-Na at the higher temperature. Such a shift was previously reported by Toulouse and Nowick for a synthetic crystal.[22] In view of the fact that any shift greater than 0.2 K is outside of experimental error, it must be concluded that all of the peaks in Fig.6 are not the same, i.e. that they are either due to different centers or, more likely, to the same center perturbed by different interactions with adjacent defects.

The following defect model is capable of explaining the principal facts associated with room temperature irradiation and subsequent annealing. When alkali ions are freed from Al-M centers, two processes, each fully charge compensated, occur: (1) M^+ may be interchanged with H^+ in the grown-in OH centers. If we call these centers G-H, the latter being produced, G-M and Al-OH centers, the latter being detected by the characteristic IR bands at 3306 and 3367 cm^{-1}. (2) The Al^{3+} ion may become separated from its alkali by capturing a hole to form Al-h, while the corresponding electron is trapped with the alkali to from neutral alkali centers at certain (thus far, unknown) defect sites in the crystal. (The latter may be somewhat different in natural and synthetic crystals.) These alkali centers are presumed to give rise to the "irradiation peak" studied here. The Al-h center is always exactly the same, as indicated by the ESR spectrum, but the alkali centers can be perturbed because they are part of a larger cluster. Annealing then occurs in two stages, as observed by Martin [19] and in this paper. Stage I, which

occurs between 450 and 550 K involves recombination of the electron and hole, to eliminate the Al-h center and the alkali center which causes the irradiation peak. the concept that electrons and holes become mobile in Stage I is also supported by the fact that the formation of E'_1 centers after irradiation (which involve an electron trapped at an oxygen vacancy) only takes place after annealing in Stage I. Stage II, which occurs between 600 and 700 K involves re-exchange of M^+ and H^+ to restore the G-OH and Al-M centers. The crystal is then restored to its as-grown condition. While the above model may too simplified, and still leaves open the question of the nature of both the G-OH centers and the trapping sites for the alkalis and electrons, it nevertheless can serve as a starting point for attempting a better understanding of irradiation processes in quartz crystals.

ACKNOWLEDGEMENT

The authors are grateful to Prof. Joel Martin for carrying out electrodiffusion on the various samples studied here. This work was supported by the U.S. Air Force under contracts F 19628-82-K-0013 and F 19628-85-C-0104 and monitored by H.G. Lipson, RADC Hanscom AFB.

REFERENCES

1. J.C. King and H.H. Sander, Rad. Effects 26, 203 (1975).
2. P. Pelligrini, F. Euler, A. Kahan, T.M. Flanagan and T.F. Wrobel, IEEE Trans. Nucl. Sci. NS-25, 1267 (1978).
3. L.E. Halliburton, N. Koumvakalis, M.E. Markes and J.J. Martin, J. Appl. Phys. 52, 3565 (1981).
4. J.C. King, Bell Syst. Tech. J. 38, 573 (1959).
5. A. Kats, Philips Res. Rep. 17, 133 (1962).
6. R.N. Brown and A. Kahan, J. Phys. Chem. Solids 36, 467 (1975).
7. H.G. Lipson and A. Kahan, J. Appl. Phys. 58, 963 (1985).
8. H. Jain and A.S. Nowick, J. Appl. Phys. 53, 477 (1982).
9. R.C. Hughes, Rad. Effects 26, 225 (1975).
10. H. Jain and A.S. Nowick, J. Appl. Phys. 53, 485 (1982).
11. E.R. Green, J. Toulouse, J. Wacks and A.S. Nowick, in Proc. 38th Ann. Symp. on Freq. Control IEEE Cat. No. 84CH2062-8, 1984, pp. 32-37.
12. J.M. Stevels and J. Volger, Philips Res. Rep. 17, 283 (1962).
13. D.S. Park and A.S. Nowick, Phys. Stat. Sol. (a) 26, 617 (1974).
14. J. Toulouse and A.S. Nowick, J. Phys. Chem. Solids 46, 1285 (1985)
15. W.J. de Vos and J. Volger, Physica 34, 272 (1967); 47, 13 (1970).
16. M.E. Markes and L.E. Halliburton, J. Appl. Phys. 50, 8172 (1980).
17. D. Adler, in Treatise on Solid State Chemistry Vol. II, edited by N.B. Hannay (Plenum Press, New York, 1975), Chap. 4.
18. T.H. DiStefano and D.E. Eastman, Phys. Rev. Lett. 27, 1560 (1971).
19. J.J. Martin, J. Appl. Phys. 56, 2536 (1984).
20. J.J. Martin, H.B. Hwang and H. Bahidur, in Proc. 39th Freq. Control Symp, IEEE, 1985.
21. L.E. Halliburton, private communication.
22. J. Toulouse and A.S. Nowick, in Defect Properties and Processing of High Technology Nonmetallic Materials, edited by J.H. Crawford et al. (North Holland, New York, 1984) pp. 149 - 157.
23. M.G. Jani, R.B. Bossoli and L.E. Halliburton, Phys. Rev. B 27, 2285 (1983).

Dielectric relaxation of the aluminum-hole center in α-quartz: An example of phonon-assisted tunneling

J. Toulouse,* S. Ling,† and A. S. Nowick
Henry Krumb School of Mines, Columbia University, New York, New York 10027
(Received 4 September 1987)

A detailed study is made of the low-temperature dielectric relaxation peak that develops in crystalline quartz upon irradiation. A wide variety of crystals are employed: from different sources, with different purities, and with the Al^{3+} impurity compensated by a selected alkali-metal ion (Li^+ or Na^+) or by H^+ through the use of the technique of "sweeping." A comparison is made between the dielectric peak height and the intensity of the well-known EPR spectrum due to the aluminum-hole (Al-*h*) center. It shows that the dielectric loss peak is due to the Al-*h* center, with the hole located on a "long-bond" oxygen atom. Analysis of the relaxation rate as a function of temperature shows that, below ~ 6 K the relaxation takes place by a one-phonon tunneling process, while above this temperature a multiphonon process occurs. While the relaxation time in the one-phonon regime is unique, the relaxation spectrum and the mean relaxation time in the multiphonon regime are sample dependent, due to phonon scattering by crystal defects.

I. INTRODUCTION

Crystalline quartz has become the foremost material in ultrasonic devices and precision frequency standards. Accordingly, there is considerable interest in the nature of point defects in quartz crystals, particularly those that can affect their frequency stability. Perhaps the most important defects in quartz are those involving an Al^{3+}-ion impurity substituting for Si^{4+}. Since the Al has a lower valence than Si, an additional positive defect is required for charge compensation. This is usually provided by an interstitial alkali ion (Li^+ or Na^+) or by protons. The alkali ion M^+ becomes bound to the Al ion by Coulombic attraction to form an Al-*M* pair, while H^+ forms an OH^- bond near the Al. The presence of the Al-OH defect is detectable by infrared measurements.[1,2] The defect structure is changed by ionizing radiation in the vicinity of room temperature. Such changes under irradiation are of interest because they are accompanied by frequency drifts of quartz resonators.[3-5]

Figure 1 schematically shows an Al^{3+} ion substituted for a Si^{4+}, sitting at the center of a distorted tetrahedron of four O^{2-} ions. The tetrahedron contains a single twofold symmetry axis, designated by C_2 in the figure. An interstitial alkali ion sits within this tetrahedron either on the C_2 axis (for Li^+) or off the axis (for Na^+).[6] Upon irradiation at a temperature above 200 K, the alkali ion is liberated and may be replaced by a hole to form the aluminum-hole (Al-*h*) center.[7] This center has a characteristic electron-paramagnetic-resonance (EPR) spectrum, and it has been widely studied by this technique.[8]

Dielectric relaxation has become an important tool in the study of defects in quartz. The pioneering work of Stevels and Volger[9] revealed a pair of dielectric-loss peaks at low temperatures that could be attributed to the Al-Na defect. They also found an additional peak at very low temperatures following irradiation, which they attributed either to the Al-*h* center or to an alkali center. A further detailed study was made of this peak in various natural "smoky quartz" crystals by de Vos and Volger.[10] In later studies carried out by some of the present authors, differences in the relaxation behavior were found among different samples, suggesting that the relaxation might be due to an alkali center rather than to the Al-*h* center; accordingly, it was referred to simply as the "irradiation peak."[11]

This paper represents an extensive study of this irradiation peak using a wide range of crystals from different sources, including natural crystals and cultured crystals of various qualities. In addition, we have made use of the technique of electrodiffusion or "sweeping"[1,3,12] to obtain samples in which the monovalent compensation for Al^{3+}

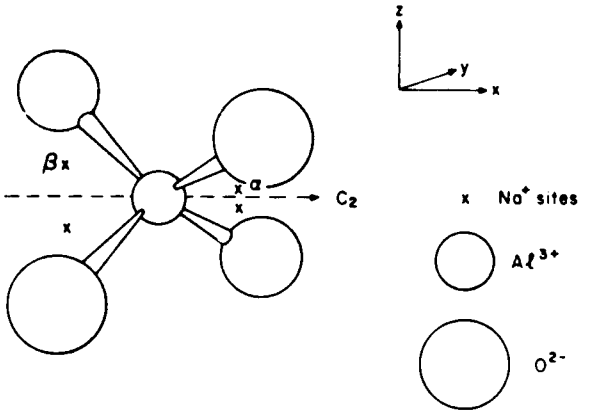

FIG. 1. Schematic diagram showing the distorted tetrahedron, the basic structural unit of α quartz, with Al^{3+} replacing Si^{4+}. The single twofold symmetry axis, designated C_2, is taken in the *x* direction. The four sites (two denoted α and two β) of an interstitial Na^+ compensating the Al^{3+} are also shown.

is primarily of one kind (i.e., Li^+, Na^+, or H^+). As a result of this work we are able to show that the "irradiation peak" is indeed produced by the Al-h center, and we investigate some of its unusual characteristics, which turn out to be related to phonon-assisted tunneling.

II. THEORY

Dielectric loss can arise from defects that have a lower point symmetry than that of the crystal in which they reside.[13,14] Such defects possess several crystallographically equivalent orientations, among which they may reorient preferentially in the presence of an electric field. If the electric field is sinusoidal with angular frequency ω, one or more peaks will usually occur in the dielectric loss, $\tan\delta$, which obey the well-known Debye equation:

$$\tan\delta=(\delta\epsilon/\epsilon_\infty)\omega\tau/(1+\omega^2\tau^2)\ , \tag{1}$$

where ϵ_∞ is the dielectric constant observed at high frequencies, $\delta\epsilon$ is called the relaxation of the dielectric constant, and τ is the relaxation time. The quantity $\delta\epsilon/\epsilon_\infty$ is often termed the relaxation strength Δ. Equation (1) yields a symmetric peak in a plot of $\tan\delta$ vs $\log_{10}\omega$ centered about the value ω_m given by

$$\omega_m=\tau^{-1}\ , \tag{2}$$

and of width at half-maximum: $\delta\log_{10}\omega=1.144$.

In α quartz, which has trigonal symmetry, the highest site symmetry is that of a Si^{4+} ion. This site is monoclinic and involves a twofold (C_2) axis which is taken along the x axis of the crystal. The Si^{4+} sits at the center of an SiO_4 distorted tetrahedron. When Al^{3+} is present, it replaces the Si^{4+} at the tetrahedron center as shown in Fig. 1. If the charge compensator is located nearby, but not on the C_2 axis, this defect pair forms an electric dipole. Such a dipole has six equivalent orientations, two on each tetrahedron, and on three differently oriented tetrahedra (each rotated through 120° and translated by $c/3$ from the other) in each unit cell. For the defect to reorient from one tetrahedron to another, however, requires the migration of the Al^{3+}. The activation energy for such a process is expected to be far too high for such a jump to take place in the temperature range of the present experiments. Accordingly, relaxation can occur only by reorientation of the pair across the C_2 axis of each tetrahedron. Nowick and Stanley[15] have shown that the relaxation of the dielectric constant under such a constraint is given by

$$\delta\epsilon_\parallel=N_d\mu_3^2/\epsilon_0 kT \tag{3}$$

when the electric field is applied parallel to the crystal c axis, and by

$$\delta\epsilon_\perp=N_d\mu_2^2/2\epsilon_0 kT \tag{4}$$

for an electric field applied in the basal plane. Here N_d is the number of dipoles per unit volume, ϵ_0 the permittivity of vacuum, kT has the usual meaning, and μ_2 and μ_3 are the components of the dipole moment along the y and z directions (the latter being parallel to the c axis). Consequently, the anisotropy ratio R_a of the maxima in $\tan\delta$, for the parallel relative to the perpendicular directions, is

$$R_a=(2\epsilon_{x\perp}/\epsilon_{x\parallel})(\mu_3/\mu_2)^2\ . \tag{5}$$

As for the relaxation time, for classical jumping over a barrier, we obtain the rate τ^{-1} in the classical Arrhenius form. Under such circumstances one can vary $\omega\tau$ in Eq. (1) by changing the temperature and keeping the frequency constant. A plot of $\tan\delta$ vs $1/T$ then gives a symmetric peak. Many "paraelectric" defects in a variety of materials have been studied, which undergo relaxation at very low temperatures with the aid of phonon-assisted tunneling.[16] Under these circumstances, one may observe a linear dependence of τ^{-1} on T in the lowest temperature range (where a single-phonon process takes place) and a power-law increase at higher temperatures (where a multiphonon process occurs):

$$\tau^{-1}=AT+BT^n\ , \tag{6}$$

where n is expected to fall in the range 4–7, depending on the detailed assumptions of the theory.[17–21] Alternatively, one may find an exponential (Arrhenius) form in the multiphonon region, to obtain

$$\tau^{-1}=A'T+\nu_0\exp(-E/kT)\ . \tag{7}$$

These equations have been applied to various "off-center," "paraelectric," and "paraelastic" defects in the past.[16]

III. METHODS

The samples used in this investigation are listed in Table I, with their label ("autoclave designation") and origin. All of them were cultured (synthetic) quartz crystals, from the various sources indicated, except for no. 8, which was a natural crystal. The cultured crystals nos. 1–5 are high-quality crystals, grown slowly so as to keep the impurity content low, while others, e.g., nos. 6 and 7, were grown rapidly and have a higher impurity content. Two samples were cut from crystal nos. 3, 5, 7, and 8 and separately electrodiffused (at Oklahoma State University) with Li and Na, respectively. Other samples were air swept; this results in the replacement of alkalis by protons.[12] The vacuum sweeping treatment of no. 2 consisted of electrodiffusing a previously air-swept sample for 52 days at 500 °C under vacuum.

The swept crystals were subjected to two kinds of irradiation, with x and γ rays. The x irradiations were performed with rays from a tungsten tube operating at 40 kV and 20 mA for 4 hours. The samples were placed against the window of the x-ray tube and irradiated through a filter consisting of a sputtered silver electrode less than 1-μm thick, and sometimes a glass plate of 1-mm thick. The soft x rays were thus eliminated and the sample homogeneously irradiated. The γ irradiation was performed at Brookhaven National Laboratory with a cobalt source. This irradiation lasted four hours to give a total dose of 4 Mrads. The irradiated samples were kept under refrigeration to minimize the effect of room-temperature annealing on the height of the dielectric-loss peak.

The irradiated samples used for the electrical measure-

TABLE I. Crystals used in this investigation. (All are cultured, except for no. 8)

Crystal no.	Autoclave designation[c]	Source	Al content (ppm)	Sweeping
1	E42-21	Sawyer	2[b]	
2	H29-14	Sawyer	4[a]	Vacuum
3	PQ-E	Sawyer	17[a]	Na, Li
4	PQ-D	Sawyer	6[a]	Air
5	SQ-A	Tokyo, Japan	13[a,b]	Na, Li, Air
6	QA26	AF, RADC	55[b]	Na
7	HA-A	USSR	352[b]	Na, Li
8	NQ	Arkansas (natural)	70[b]	Na, Li

[a]From EPR measurements (Ref. 7).
[b]From the Al-Na α peak (Ref. 6).
[c]Samples from most of these crystals have been used in previous studies (Refs. 2, 6, 7, 11, and 22) where the same designations were employed.

ments were approximately $1\times1\times0.18$ cm^3, with the thin dimension along the z axis of the crystal. Electrical contacts with the samples were made via two silver electrodes. A full electrode was sputtered on one side of the sample, and a central electrode painted on the other with Engelhard flexible silver paint no. 16. A guard ring was also painted circling the central electrode. It was grounded to prevent surface conduction between the two electrons resulting from fringe field effects.

The samples were transferred to a Janis SuperVari-Temp cryostat and cooled down to liquid-helium temperature. Two samples were simultaneously placed in the cryostat, one on top of the other, separated by a 1.5-mm thick sapphire disk. The temperature was monitored via a Lake Shore silicon diode sensor embedded in a copper block just below the samples. The temperature uncertainty was ±0.1 K above 4.8 K and about ±0.15 K below 4.8 K.

The dielectric measurements were carried out with a General Radio capacitance bridge 1615A automated by Carl Andeen Inc. with a constant signal generator output of 5 V. The measurements covered a frequency range of 10 Hz–100 kHz and a temperature range of 3–100 K.

IV. RESULTS

A wide variety of samples was studied in this work, including both natural and cultured crystals, samples with high and low Al^{3+} content, Na^+-, Li^+-, and H^+-swept samples and vacuum-swept samples. For almost all of the samples studied, the low-temperature "irradiation peak" was observed following x-ray or γ-ray irradiation, and not before irradiation. The only exception to this statement is the vacuum-swept sample which showed a small peak without any irradiation.

The irradiation peak was studied in detail by making rapid measurements at 17 frequencies (from 10 Hz to 100 kHz) utilizing the automated ac bridge, at each temperature, while varying the temperature between ~3 and 80 K. The data were first plotted in the traditional manner as a function of T^{-1} (where T is the Kelvin temperature) for the various frequencies. A typical example is given in Fig. 2 for an irradiated no. 5 Na-swept crystal. (For clarity, not all of the frequencies are included.) It is noteworthy that the peaks, particularly those for the lower frequencies, become highly asymmetrical on the low-temperature side, in contrast to the symmetry peak

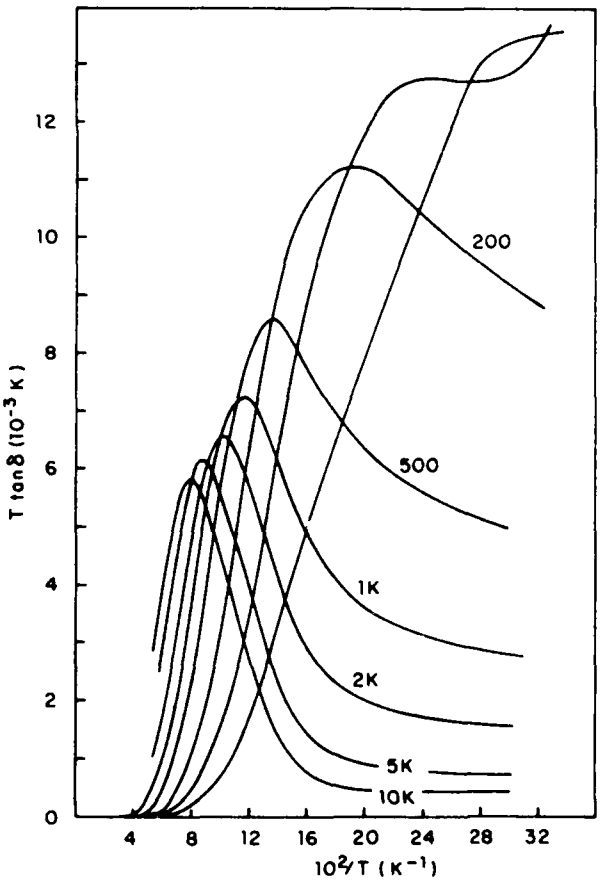

FIG. 2. Plot of $T\tan\delta$ as a function of reciprocal temperature at various frequencies of measurement (from 200 Hz to 10 kHz) for sample no. 5 (Na swept) after x irradiation.

predicted by Eq. (1) combined with the Arrhenius equation for τ^{-1}. The same data were then calculated as a function of circular frequency ω and plotted versus $\ln\omega$, as illustrated in Fig. 3. The range of the plot is limited by the frequency range of the apparatus, but it is clear that the peaks are narrow and symmetrical for the lower temperatures and become broader and asymmetrical at the higher temperatures. The advantage of the frequency plots is that they can be analyzed without any assumption about the form of the dependence of τ^{-1} on T, and therefore permit a more direct test of the Debye equation (1). In fact, the peaks at the lower temperatures are very close to Debye peaks, as we shall show later. For each peak of Fig. 3, a mean relaxation rate τ^{-1} can be obtained from Eq. (2).

The relaxation rates so obtained may be studied as a function of temperature. The plot of $\log_{10}\tau^{-1}$ vs T^{-1}, which seeks an Arrhenius relation, is shown in Fig. 4 for some of the samples. Clearly, the Arrhenius relation is only obeyed reasonably well at the higher temperatures. Typical activation energies obtained are ~ 5–7 meV with preexponentials $\nu_0 \sim 10^7$ sec^{-1}. The lines on this figure show the fit to Eq. (7). Alternatively, we may seek a power-law dependence of the relaxation rate on temperature by plotting $\log_{10}\tau^{-1}$ vs $\log_{10}T$, as shown in Fig. 5.

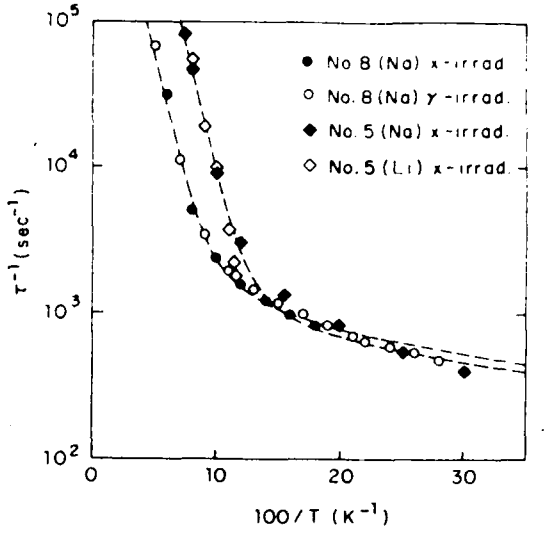

FIG. 4. Values of τ^{-1} (obtained from the peak locations of plots such as Fig. 3) as a function of reciprocal temperature for two-high quality cultured samples (no. 5) and two natural samples (no. 8). For crystal no. 5 we compare Li swept and Na swept. For crystal no. 8 we compare two different irradiations that gave peak heights differing by a factor of 4. The drawn-in curves are the best fits to Eq. (7).

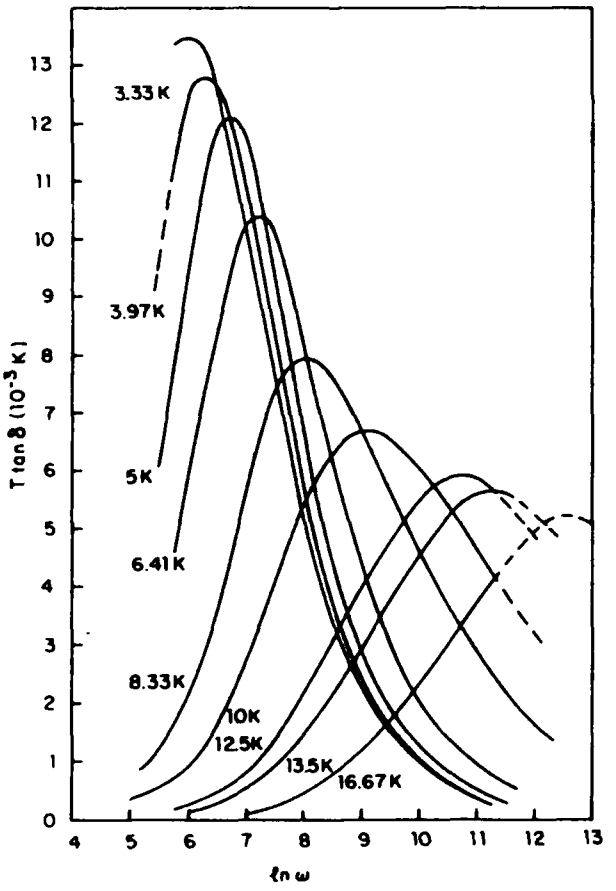

FIG. 3. Same data as Fig. 2 but plotted vs $\ln\omega$ for different temperatures from 3.33 to 16.67 K.

The results are consistent with an nth power dependence at the higher temperatures, where n ranges from 4 to 7 for different samples, and a first power dependence at the lower temperatures, in accordance with Eq. (6). The drawn-in lines represent the fit to Eq. (6). In general, we find that the break from the single phonon to the multiphonon range occurs sooner (i.e., at a lower temperature) for the higher-quality crystals (e.g., nos. 3 or 5), and later for crystals with high impurity contents (e.g., nos. 7 and

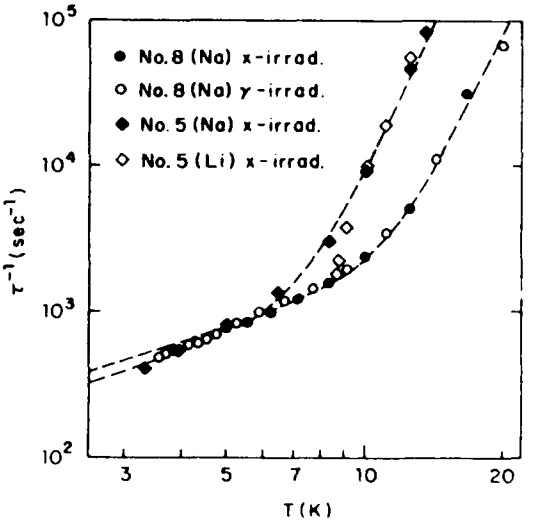

FIG. 5. The same data as in Fig. 4 plotted as $\log_{10}\tau^{-1}$ vs $\log_{10}T$. The drawn-in curves are the best fits to Eq. (6).

8). An important result, illustrated in Figs. 4 and 5, is that, whereas the relaxation rates for all of the samples are in agreement in the single-phonon range at 6 K and below, in the higher temperature range there are striking differences in τ^{-1} among different samples.

This conclusion is brought out even more strikingly in Figs. 6 and 7. Figure 6 shows the normalized peaks at 5 K for a wide variety of samples, with a theoretical Debye curve drawn in as the solid curve. It shows that the relaxation rate at 5 K is the same, to within experimental error for all of these samples and that the relaxation behavior deviates very little from a Debye process. Since the temperature of 5 K is well within the single-phonon region we conclude that the single-phonon-assisted tunneling process is a very simple one. It is also concluded that the defect involved must be one and the same for all of the samples, i.e., that there is no evidence for any perturbations due to the type of alkali present or to the magnitude of the Al concentration. In other words, the relaxation is produced by a simple isolated defect that is present in all of these samples.

By contrast, Fig. 7 shows the same type of normalized plot for the same samples at 12.5 K. Now the peak locations are all different, as is the extent of broadening and the asymmetry of the broadening for the various samples. From Fig. 5 we see that 12.5 K falls in the multiphonon range. Clearly, we must say that in this range the relaxation process is sample dependent. This can only mean that it is dependent on the presence of defects in the crystal. It is interesting that the peaks in Fig. 7 are less broadened and less asymmetric for the lower-purity crystals, i.e., those that remain in the single-phonon range to higher temperatures.

In view of these unusual results, we have raised the question of whether the 5- and 12.5-K peaks may be different relaxation phenomena. A good test of this proposal is to see how the relaxation strength Δ varies as a function of temperature. The precise way to obtain relaxation strength, especially when peak broadening occurs, is to obtain the areas under the peak. This is difficult to do in the present case because of the lack of data in the

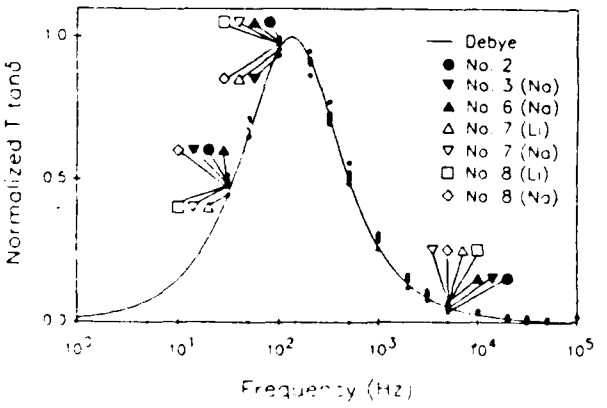

FIG. 6. Normalized dielectric-loss peaks as measured at 5 K for several samples. The curve drawn is the theoretical Debye curve [Eq. (1)].

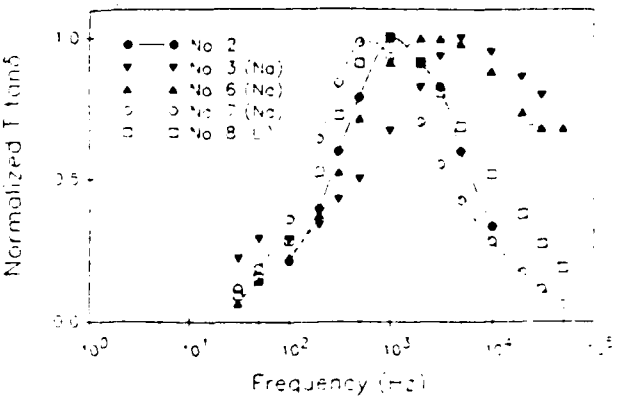

FIG. 7. Normalized dielectric-loss peaks measured at 12.5 K for several samples. The peaks are now asymmetric and considerably wider than a Debye peak.

tails of the peaks due to the limited frequency range. Instead, we have approximated the relaxation strength by taking the peak height multiplied by the width at half-maximum. Since the peaks are asymmetric we have separately measured the half-peak widths on both the high-frequency and low-frequency sides. Figure 8 illustrates the results for the sample no. 8 (Li). It shows that whereas the peak height decreases rapidly with increasing temperature, the width increases so as to compensate. Thus, the product of height and width remains constant, to within experimental error, over the entire temperature range of the measurements, including both the single-phonon and multiphonon regions. These results seem to eliminate any doubt that the same defect relaxation process is occurring at 12.5 K as at 5 K, but indicate that only the kinetics of the process are drastically different at these two temperatures.

Table II gives a summary of the principal results obtained for representative samples that we have studied as a function of temperature and frequency in the manner of Figs. 3–5. Included are the parameters obtained by computer fitting the data for the variation of τ^{-1} with temperature to Eq. (6) (parameters A, B, and n) and to Eq. (7) (parameters A', ν_0, and E). The low-temperature parameters, A or A', are not very sensitive to the different samples or to the fitting procedure, but the higher-temperature parameters are more sensitive to these factors. The uncertainty in the fitting of n is approximately ± 0.5, while that of E is ± 0.5 meV. A convenient way of comparing where each sample falls in a plot of the type of Fig. 4 or 5 is to quote τ^{-1} at 10 K, as given in the last column of Table II. These values are high for the high-quality crystals nos. 1, 3, and 5, consistent with their early transition from the single to the multiphonon region, and low for the more impure crystals, particularly nos. 7 and 8. What is particularly striking is that, for a given crystal, this value of τ^{-1} is almost the same for widely different radiation doses (and, therefore peak heights) and for Na versus Li sweeping. It must be concluded that the values of τ^{-1}, and therefore the single-phonon to multi-

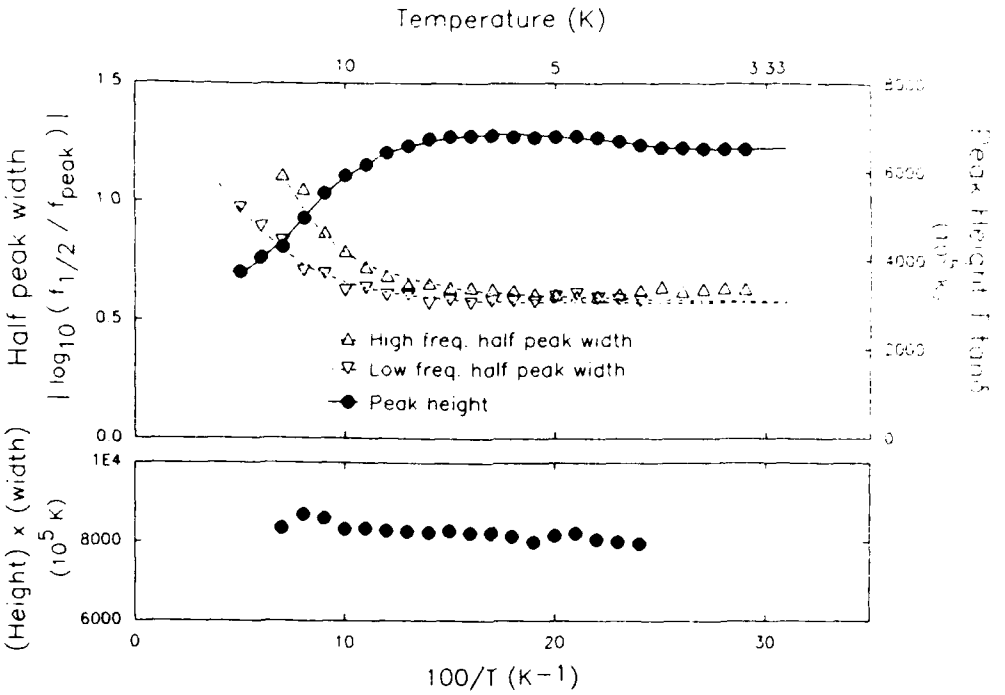

FIG. 8. Upper plot: Variation of peak height, $T\tan\delta_{max}$, and of peak width on both the low-frequency and high-frequency sides, as a function of temperature for No. 8 (Li) sample γ irradiated for 4 h. Lower plot: Product of (height)×(width) from the above data as a function of temperature.

phonon transition, are controlled by defect properties created in each sample during the growth process rather than the radiation dose or the nature of the impurity compensating for Al^{3+}.

Thus far, we have concentrated mainly on the kinetic aspects (i.e., on τ^{-1}) of the relaxation. There are a number of further observations concerning the relaxation strengths that are worth stating. In general, the peak height is nearly the same for Li-swept and Na-swept samples from the same crystals. Hydrogen sweeping is different, however, in that the peak is much smaller. Thus, for example, while the 5-K peak heights for the Li or Na swept no. 3 crystal are about 260, the values for no. 4 which is from the same growth batch but air swept (by Sawyer Research Products Inc.) is only about 10 (all in units of 10^{-5}).

Another important result concerns the anisotropy ratio R_a, Eq. (5). This ratio was carefully measured, by comparing two samples from crystal no. 1, in the parallel and perpendicular orientations, respectively, after both were given identical irradiations. The experimental value was $R_a = 0.90$. The consequence of this result will be con-

TABLE II. Summary of representative results for relaxation rates. (All samples are oriented parallel to the c axis except for no. 1 ⊥). Parameters A, B, n and A', ν_0, E are obtained by fitting to Eqs. (6) and (7).

Sample No.	Treatment	$T\tan\delta_{max}$ at 5 K (10^{-5} K)	A (sec K)$^{-1}$	B (sec^{-1}K^{-n})	n	A' (sec K)$^{-1}$	ν_0 (sec^{-1})	E (meV)	τ^{-1} at 10 K (10^3 sec^{-1})
1	γ irr., 4 h	400	120	1.2×10^{-1}	5.3	140	2×10^{7}	4.5	25
1 (⊥)	γ irr., 4 h	440	155	3.4×10^{-1}	6.4	160	8×10^{6}	5.5	14
2 (vacuum)		340	145	3.6×10^{-2}	4.7	180	1.4×10^{6}	5.9	3.4
3 (Na)	γ irr., 4 h	1120	135	8.6×10^{-3}	6.0	145	5×10^{6}	5.5	16
3 (Li)	γ irr., 4 h	1460	135	5.0×10^{-3}	6.5	145	1×10^{7}	5.3	20
5 (Na)	x irr., 4 h	1215	130	8.0×10^{-4}	7.0	140	4.3×10^{7}	7.4	10
6 (Na)	γ irr., 4 h	3400	129	1.1×10^{-1}	4.6	144	7×10^{5}	4.2	4.5
7 (Na)	γ irr., 4 h	10 100	145	4.2×10^{-2}	4.5	150	5×10^{5}	5.8	2.2
7 (Li)	γ irr., 4 h	10 500	145	1.1×10^{-2}	5.4	150	2×10^{6}	5.6	3.3
8 (Na)	x irr., 4 h	1740	156	1.2×10^{-4}	6.8	158	4×10^{6}	7.3	2.5
8 (Na)	γ irr., 4 h	7220	156	1.2×10^{-4}	6.8	158	4×10^{6}	7.3	2.5
8 (Li)	γ irr., 4 h	6780	153	1.2×10^{-4}	6.9	155	6×10^{6}	7.5	2.5

sidered in the next section.

An interesting result that follows from data such as that in Fig. 8 is that $T\Delta$ is constant down to ~ 3 K. But this result is simply Curie's law for the relaxation process, i.e., that $\Delta \propto T^{-1}$. The third law of thermodynamics requires, however, that $\Delta \to$ const as $T \to 0$, or that $T\Delta \to 0$. Clearly from Fig. 8, there is not yet any evidence for this limit at 3 K. This result contrasts with that reported by de Vos and Volger.[10]

Considering our earlier conclusion that the present "irradiation peak" must be due to a simple isolated point defect that is present in all of these samples, the most reasonable candidate that suggests itself is the aluminum-hole (Al-h) center, which is known to be present in irradiated α quartz.[7] Since the Al-h center is identifiable in terms of its characteristic EPR spectrum, we selected several of the samples studied herein to be EPR analyzed. In each case, the EPR samples were taken from the central region of the samples used for dielectric-loss measurements. This was done to ensure that both EPR and dielectric-loss measurements were made on the same sample and thus minimize the discrepancy that could arise from an inhomogeneity in the defect concentration in the crystal. On the other hand, these samples were subject to some room-temperature annealing during transportation, which can cause a small decrease of the irradiation peak. Included among the samples selected was the vacuum-swept sample, the only one that showed an "irradiation peak" without irradiation. Indeed, this sample also showed an EPR signal due to the Al-h. Infrared measurements showed that all of the OH^- bands were absent in this sample, even though it had been previously H swept. This suggests that, as protons (H^+) were swept out, holes were introduced into the sample during the vacuum sweeping to compensate for the aliovalent charge on the Al^{3+}.

A summary of the results of this comparison is given in Fig. 9. Here we have plotted the height of the 5-K dielectric peak as a function of the strength of the EPR signal. (The latter is converted to a concentration of Al-h in ppm, however, using an earlier calibration).[7,22] Because of the wide range of Al-h concentrations covered, the relationship shown in Fig. 9 is given in the form of a log-log plot. The straight line drawn (with slope $=1$), representing a direct proportionality of the dielectric peak height to the EPR signal, agrees with the data to within experimental error. Considering the variety of samples and the wide range of peak heights involved in Fig. 9 (covering a factor ~ 30), it seems reasonable to conclude that the "irradiation peak" height is indeed proportional to the Al-h center concentration. Figure 9 also gives a calibration constant for the height of the 5-K peak, as follows:

$$1 \text{ ppm of Al-}h \leftrightarrow T\tan\delta_{max} = 60 \times 10^{-5}.$$

Further evidence for the close relationship between the height of the dielectric-loss peak and the Al-h EPR spectrum comes from an annealing experiment. Although we are not dealing with the annealing behavior of these centers in the present paper, it is noteworthy that, following the anneal of an irradiated sample at 230 °C for $\frac{1}{4}h$, both the dielectric peak and the EPR signal (both measured on the same sample) were found to have fallen to almost precisely half the values that they had in the initial irradiated condition.

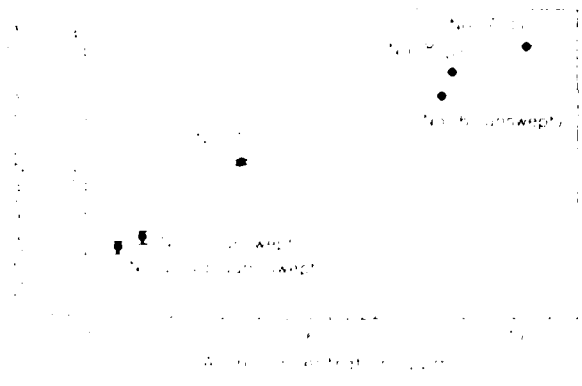

FIG. 9. Log-log plot of dielectric peak height, $T\tan\delta_{max}$ at 5 K vs strength of Al-h EPR signal (converted to Al-h concentration through a previous calibration). The straight line drawn represents a direct proportionality between these two quantities.

V. DISCUSSION

The suggestion that the low-temperature dielectric-loss peak is due to aluminum-hole (Al-h) centers was made by Taylor and Farnell[23] and by de Vos and Volger,[10] but further study of this peak showing its complexity and its variation from sample to sample had led us to question this assignment.[11] In the present work, however, the discovery of the uniqueness of the peak as measured at 5 K, as well as the comparison of its magnitude with that of the EPR signal showing the linear relationships given by Fig. 9, seems to leave no serious doubt that the dielectric peak originates in Al-h centers. The fact that the peak is much lower in hydrogen-swept samples is consistent with the demonstrated predominance of Al-OH centers over Al-h centers in H-swept samples irradiated at room temperature.[22]

Figure 1 shows that there are four oxygen ions about a substitutional Al, which are equivalent in pairs, as a consequence of the C_2 axis of symmetry. These are commonly referred to as the short-bond and long-bond oxygens (with Si-O distances of 1.608 and 1.613 Å, respectively in the perfect crystal.) EPR studies have shown that, in the Al-h center at cryogenic temperatures, the hole resides on the nearest-neighbor oxygen ion that forms a long bond with the substitutional Al.[24] It must then be concluded that dielectric relaxation takes place by reorientation of the hole between the two long-bond oxygens.

An opportunity to check this conclusion comes from the anisotropy ratio, R_a as measured on crystal no. 1 (see Table II). Equation (5) gives an expression for this ratio in terms of the ratio of dipole components μ_3/μ_2. This, in turn, is just the ratio of coordinates x_3/x_2 of the oxygen on which the hole resides (taking the Al^{3+} at the origin.) From the experimental value, $R_a = 0.90$, we obtain

$x_1/x_2 = 0.68$. Although the bond lengths are perturbed by the introduction of the hole and the substitution of Al^{3+} for Si^{4+}, if we assume that the angular relationships of the bonds are very nearly unaltered, we may use the oxygen coordinates in the perfect lattice to calculate x_1/x_2. On this basis, and using the crystallographic data in Wyckoff,[25] we calculate 0.56 for this ratio for the long-bond oxygens, a result that may be regarded as representing reasonably good agreement with the experimental values considering both the assumptions made and the experimental uncertainty. On the other hand, if the hole were on the short bond, a ratio of 1.9 would be calculated, which is quite unacceptable. Thus, the anisotropy result provides further support for the fact that the hole resides on the long Al-O bonds.

Another interesting calculation is to make use of Eq. (3) and our present calibration of the peak height in terms of the Al-*h* concentration, to obtain the component μ_1 of the effective dipole moment. When the appropriate numbers are substituted, we obtain $\mu_1 = e \times 0.5$ Å, where e is the electronic charge. This is quite a reasonable result, considering that the relaxing hole is located along the Al—O long bond.

A particularly interesting feature of the present Al-*h* relaxation concerns the changeover, with increasing temperature, from a one-phonon to a multiphonon process. Let us first say that the mere existence of such a changeover is not surprising, since such behavior has been widely observed for other dipole systems that relax at very low temperatures.[16] What is unusual here is the demonstration that, whereas the relaxation process is a unique simple Debye process in the one-phonon regime, it becomes much more complex, as well as sample (defect) dependent, in the multiphonon regime. There are two types of multiphonon processes that may be considered, viz., Orbach and Raman.[26] In the Orbach process, the transition occurs through a real excited state and results in τ^{-1} obeying an Arrhenius equation (7) with E as the excitation energy. In the Raman process, the transition occurs through a virtual state, and a T^n power law [as in Eq. (6)] is obtained. Since E is not found to be constant for the various samples (see Table II), as would be expected for an Orbach process, while n values fall in the range 4–7, consistent with various theoretical approaches,[17–21] it seems more likely that Raman processes are involved here. A qualitative interpretation of the present results may be given as follows. At the lowest temperature only a one-phonon tunneling transition can produce reorientation of the hole between the pairs of long-bond oxygen sites. This is a unique process, and thus results in a unique single relaxation time for all samples. As the temperature increases, shorter wavelength (or higher wavenumber) phonons are excited, increasing the probability of a Raman two-phonon process. Such a process can involve a shorter relaxation time than the one-phonon process, but since many different combinations of phonons can induced the transition, it no longer involves a unique relaxation time. Thus, the broadening of the peak, as shown in Fig. 7, occurs. In addition, however, such phonons of relatively high wave number are also more susceptible to scattering by crystal defects (both point defects and dislocations). The occurrence of such scattering interferes with the multiphonon process and thus accounts for the large variation in τ values among different samples, as shown in Figs. 4 and 5 and in Table II. The fact that the more impure crystals (nos. 7 and 8) remain longer, i.e., to higher temperatures, in the single-phonon regime supports this interpretation. Further evidence for the scattering of phonons by defects is obtained from thermal-conductivity measurements. Such measurements show that crystals containing point defects have a lower thermal-conductivity maximum (near 10 K), due to the decrease in the phonon mean free path produced by defect scattering.[27]

It would be interesting to see if the present observations of defect sensitivity of the multiphonon process for the Al-*h* center in quartz can also be observed for other tunneling dipoles (e.g., Li^+ in KCl, OH^- in alkali halides, etc.). Such experiments could be carried out by studying the dependence of τ^{-1} vs T in a series of samples that have been deliberately doped with another impurity.

In summary, the principal results of the present study show (i) that the low-temperature "irradiation peak" is produced by the aluminum-hole center, (ii) that below ~6 K the relaxation of the hole between the two long-bond oxygens takes place by a one-phonon process, and above this temperature by a multiphonon process, and (iii) that the relaxation kinetics in the multiphonon range are strongly sample dependent, due to the role of crystal defects in producing phonon scattering.

ACKNOWLEDGMENTS

The authors are grateful to J. J. Martin for the sweeping experiments, to L. E. Halliburton for the EPR measurements, and to H. G. Lipson for the vacuum-swept samples and for infrared measurements carried out upon them. Thanks also go to G. D. Watkins, W. B. Fowler, and F. Ham for helpful discussions. This work was supported by the U.S. Air Force under Contract No. F 19628-85-C-0104 monitored by H. G. Lipson, RADC Hanscom Air Force Base.

*Present address: Department of Physics, Lehigh University, Bethlehem, PA 18015.

†Present address: Exxon Research and Engineering Laboratory, Annandale, NJ 08801.

[1] A. Kats, Philips Res. Rep. **17**, 133 (1962).

[2] H. G. Lipson and A. Kahan, J. Appl. Phys. **58**, 963 (1985).

[3] J. C. King, Bell Syst. Tech. J. **38**, 572 (1959).

[4] B. R. Kapone, A. Kahan, R. N. Brown, and J. R. Buckmelter, IEEE Trans. Nucl. Sci. **NS-13**, 130 (1966).

[5] J. C. King and H. H. Sander, Radiat. Eff. **26**, 203 (1975).

[6] J. Toulouse and A. S. Nowick, J. Phys. Chem. Solids **46**, 1285 (1985).

[7]M. E. Markes and L. E. Halliburton, J. Appl. Phys. **50**, 8172 (1979).
[8]L. E. Halliburton, Cryst. Lattice Defects Amorph. Mater. **12**, 163 (1985).
[9]J. M. Stevels and J. Volger, Philips Res. Rep. **17**, 283 (1962).
[10]W. J. de Vos and J. Volger, Physica (Utrecht) **34**, 272 (1967); **47**, 13 (1970).
[11]J. Toulouse and A. S. Nowick, in *Proceedings of the Materials Research Society Symposium*, edited by J. H. Crawford *et al.* (Elsevier, New York, 1984), Vol. 24, p. 149.
[12]J. J. Martin, J. Appl. Phys. **56**, 2536 (1984).
[13]A. S. Nowick and W. R. Heller, Adv. Phys. **14**, 101 (1965).
[14]A. S. Nowick, Adv. Phys **16**, 1 (1967).
[15]A. S. Nowick and M. W. Stanley, in *Physics of the Solid State*, edited by S. Balakrishna *et al.* (Academic, New York, 1969), p. 183.
[16]F. Bridges, Crit. Rev. Solid State Sci. **5**, 1 (1975).
[17]J. A. Sussman, Phys. Kondens. Mater. **2**, 146 (1964).
[18]J. A. Sussman, J. Phys. Chem. Solids **28**, 1643 (1967).
[19]R. Pirc, B. Zeks, and P. Gosar, J. Phys. Chem. Solids **27**, 1219 (1966).
[20]B. G. Dick and D. Strauch, Phys. Rev. B **2**, 2200 (1970).
[21]H. B. Shore and L. M. Sander, Phys. Rev. B **6**, 1551 (1972).
[22]L. E. Halliburton, N. Koumvakalis, M. E. Markes, and J. J. Martin, J. Appl. Phys. **52**, 3565 (1981).
[23]A. L. Taylor and G. W. Farnell, Can. J. Phys. **42**, 595 (1964).
[24]R. H. D. Nutall and J. A. Weil, Can. J. Phys. **59**, 1696 (1981).
[25]R. W. G. Wyckoff, *Crystal Structures* (Wiley, New York, 1965), Vol. 1.
[26]See, for example, A. Abragam and B. Bleaney, *Electron Paramagnetic Resonance of Transition Ions* (Oxford University Press, London, 1970), Chap. 10.
[27]J. W. Vandersande and C. Wood, Contemp. Phys. **27**, 117 (1986).

DIELECTRIC RELAXATION AND EPR IN QUARTZ CRYSTALS CONTAINING Fe

S. Keilson, S. Ling and A.S. Nowick
Henry Krumb School of Mines, Columbia University
New York, NY 10027

and

L.E. Halliburton
Physics Department, Oklahoma State University
Stillwater, OK 74078

Summary

Iron-doped quartz, notably cultured amethyst, has been studied by combining the techniques of dielectric relaxation (DR) and electron spin resonance (ESR) on the same samples. In addition, samples examined were swept with Na^+, Li^+ and H^+. The DR results show four new relaxation peaks (at 20, 99, 138 and 195 K for a 1 kHz frequency) two of which (20 and 138 K) appear only for Na-swept samples. The ESR measurements show three centers S_1, S_2 and S_3. The S_1 center is believed to be due to substitutional Fe^{3+} with an adjacent interstitial Li^+ ion, while the S_2 is due to an Fe-OH center. On the other hand, the S_3 spectrum, which apparently has not been reported previously, is due to Fe-Na pairs, and is related to the 20 K and 138 K DR peaks. It appears that the S_1 and S_2 centers do not have DR equivalents. Accordingly, the 99 K and 195 K DR peaks may be related to Fe in a valence state other than 3+.

Introduction

It is well known that impurities and point defects play a large role in determining the properties of α-quartz, and thus determine its usefulness for precision frequency control in electronic devices.[1,2] There has been a long-standing interest in the effects of Fe in quartz, particularly in view of the naturally occurring forms of amethyst and citrine. In spite of a large number of studies, however, it can be said that we know relatively little about defects involving Fe as an impurity compared, for example, to those involving Al. In fact, with the aid of a wide ranges of techniques (especially infrared absorption, dielectric and anelastic relaxation and electron spin resonance: ESR) it has been found that Al^{3+} ions substitutionally occupy Si^{4+} sites at the center of a distorted tetrahedron of O^{2-} ions (see Fig. 1), and that the Al^{3+} ion is charge compensated by either an interstitial alkali (Li^+ or Na^+) or a proton (H^+). In this way centers called Al-Li, Al-Na or Al-OH are formed, the latter designation because the proton resides on one of the adjacent O^{2-} ions forming an OH ion. Finally, irradiation at room temperature can drive off an alkali and replace it with an electron hole to obtain the aluminum-hole, Al-h, center. The case of Na compensation (Al-Na center) is especially interesting, since the Na^+ ion resides off the 2-fold symmetry axis (denoted by C_2 in Fig. 1) in one of two sets of equivalent sites (denoted by α and β in Fig. 1). This defect then gives rise to two dielectric relaxation peaks, one due to the α sites, the other to the β sites, and similarly it gives rise to a pair of anelastic (internal friction) peaks.[3,4] In the case of the Al-Li defect, the Li^+ ion sits on the C_2 axis and, therefore, produces no such relaxation peaks.[3]

The Fe^{3+} ion differs from Al^{3+} in several important ways. First, it has a larger ionic radius than Al^{3+} and therefore is much larger (by ~ 50%) than the Si^{4+} ion. Second, it can change valence under irradiation conditions, while Al^{3+} probably does not. Finally, it possesses a half-filled 3d shell ($3d^5$), so that, unlike the Al^{3+} ion, it is paramagnetic and gives rise to a strong ESR spectrum. This allows one to obtain information about its crystal site and nearby defects. Thus, in contrast to Al-containing quartz, where ESR signals can only be observed following irradiation, ESR has provided the principal technique for the study of Fe-containing quartz.[5] A brief review of the literature shows that four distinct ESR spectra have received major attention. The first of these to be characterized was the S_1 center.[6,7] This defect apparently consists of an Fe^{3+} ion substituting for a Si^{4+} with an adjacent interstitial Li^+ ion providing the needed charge compensation. A similar Fe^{3+} ESR spectrum, except with a larger crystal field splitting and a weak hyperfine splitting due to an I = 1/2

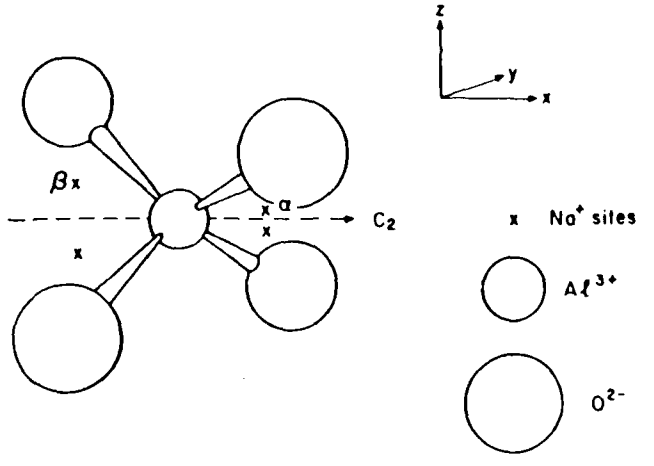

Fig. 1. Schematic diagram showing the distorted tetrahedron, the basic structural unit of α-quartz, with Al^{3+} replacing Si^{4+}. The tetrahedron contains a single twofold symmetry axis (in the x direction) designated C_2. Also shown are the two equivalent α-sites and the two equivalent β-sites. An interstitial Na^+ compensating the Al^{3+} will go into one of these four sites.

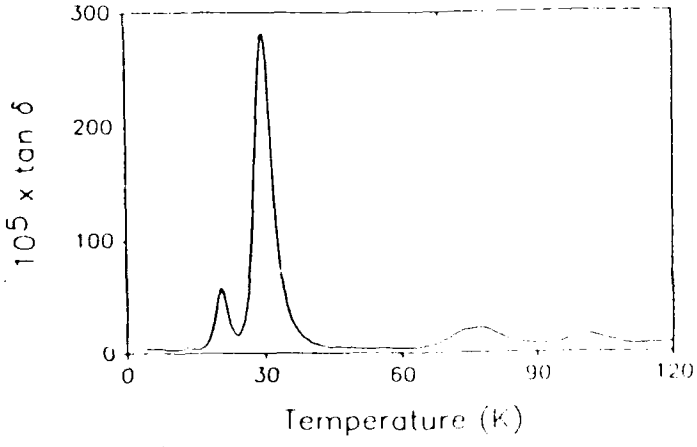

Fig. 2. Dielectric loss, tan δ, at 1 kHz as a function of temperature from 3 to 120 K for a Na-swept amethyst sample.

nucleus, has been designated the S_2 center.[8,9] This defect is a substitutional Fe^{3+} with an adjacent proton, in the form of an OH^- ion, providing the charge compensation.

A third Fe^{3+} spectrum that has been widely studied is the so-called I center.[10,11] There is significant debate over whether the I center is an interstitial or a substitutional Fe^{3+} ion. In either case, the charge compensation mechanism remains unidentified. A final ESR spectrum of importance has been reported by Cox.[13] It is assigned to Fe^{3+} ions and is directly related to the amethyst color itself.

The objective of the present work is to carry out a study of Fe-doped quartz using the combination of dielectric relaxation and ESR techniques on the same (cultured) samples. In addition, the technique of electrodiffusion (sweeping)[14,15] is used so as to introduce, as much as possible, only a single alkali or hydrogen as the principal compensator for both Al^{3+} and Fe^{3+} in a given sample. Because of these two features: the simultaneous use of two different techniques, and the control over the monovalent compensator, it is hoped that a fuller picture of Fe defects in quartz would emerge from the present work than had hitherto been obtained.

Experimental Methods

Two samples of cultured amethyst obtained from Sawyer were availble for study. They were both grown with rhombohedral seeds. The second of these was a large crystal that was oriented so that samples could be cut parallel to the c-axis. Such samples were then suitable for sweeping, which was carried out by J.J. Martin at Oklahoma State University. The samples were generally 1.0 cm^2 and 1-2 mm thick, with the thin dimension parallel to the c-axis. In addition to sweeping, samples from both crystals were subjected to irradiation and anneal treatments.

Samples for dielectric studies were irradiated at room temperature with x-rays from a tungsten target source operated at 20 mA and 40 kV. Soft x-rays were filtered out by a layer of sputtered silver electrode, and a glass filter. Other samples were irradiated at room temperature with Y-rays from a Co source at Brookhaven National Laboratory, to a total dose of 2 Mrads.

For dielectric measurements, the samples were transferred to a Super Varitemp Cryostat (Janis Corp). and cooled down to liquid helium or liquid nitrogen temperatures. An automated capacitance bridge (Andeen Assoc.) was use to carry out the dielectric loss measurements. The measurements cover a frequency range of 10Hz to 100 kHz and a temperature range of 3-270 K.

Electron spin resonance (ESR) data were obtained from a Bruker ER200D spectrometer. The microwave frequency was 9.3 GHz and the modulation frequency was 100 kHz. All the ESR spectra described in this paper were taken at 27 K using an Oxford Instruments liquid helium flow system. Dimensions of the ESR samples were approximately 2 x 3 x 7 mm^3, and the magnetic field was always aligned parallel to the crystal's c axis (i.e., the smallest dimension). The ESR samples were also irradiated at room temperature with 2-MeV electrons from a Van de Graaff accelerator.

Results and Discussion

Dielectric Relaxation (DR)

Swept samples were either Na- or Li- swept, or swept in air to eliminate alkalis and substitute H^+ (designated H-swept). The most interesting results were obtained for the Na-swept samples. Figure 2 shows the dielectric loss plot for a Na-swept sample in the temperature range from 3 to 110 K, while Fig. 3 shows the results for all three sweepings in the higher temperature range 80 to 220 K. First it should be noted that the Na-swept sample shows the well-known peaks at 30 K and 75 K due to the Al-Na center. (All peak temperatures are quoted for a frequency of 1 kHz.) From the height of the 30 K peak and the previous calibration of this peak,[7] it is concluded that the

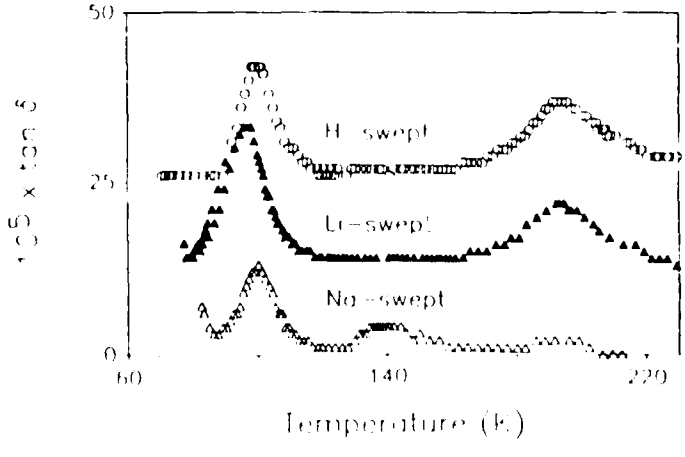

Fig. 3. Comparison of dielectric loss for Na-, Li- and H-swept amethyst in the intermediate temperature range. For clarity, the two upper curves have been displace upwards.

Table 1. Heights of Fe-related Dielectric Loss Peaks in Amethyst Samples Given Different Treatments
(Peak heights in units tan δ_{max} of 10^{-5})

Sample and Treatment	20K	99K	138K	195K
As rec'd (Ann.)	-	15	-	10
As rec'd (Y-Irr.)	-	9	-	63
H-swept	-	16	-	10
H-swept (Y-Irr.)	-	13	-	25
Li-swept-A	-	20	-	8
Li-swept-B	-	17	-	3
Na-swept-A	58	11	4	-
Na-swept-B	90	10	6	-
Na-swept-B (Y-Irr.)	<1	4	1	-

concentration of Al-Na centers is 130 ppm, a rather large Al concentration. Second, it should be noted that there are two unique new peaks in the Na-swept amethyst, those at 20 K and 138 K, respectively. Third, there is a peak at 99 K that occurs for all three swept samples. This peak is ubiquitous for Fe-doped samples, and has been observed as well in citrine samples. Finally, there is a peak at 195 K only for the Li-swept and H-swept samples. A summary of all of these results is presented in Table 1 which gives the heights of all of these peaks. At the same time, Table 2 gives the activation energy, E, and pre-exponential, ν_o, for each peak, as obtained from the shift of the peak with changing frequency, ω.

All of these peaks are very close to Debye peaks, and therefore must be produced by simple point defects. Some additional peaks have been observed at still higher temperatures, but since these are very large and not always reproducible, it is concluded that they may arise from second-phase particles and interfaces.

The only additional peak produced by irradiation in all of these samples is the low temperature peak near 10 K. This is the peak that has been studied in detail and is now established to be due to the aluminum-hole (Al-h) center.[15,16] Thus, there is no new irradiation peak due to iron. The absence of an analog to the Al-h center for Fe can be explained by realizing that Fe^{3+} can change valence (to Fe^{4+}) when it captures a hole, rather than forming a dipole by having the hole on an adjacent oxygen ion, as in the case of Al^{3+}. Irradiation does, however, change the heights of the other Fe-related peaks, as shown in Table 1. Interestingly enough, the 20, 99 and 138 K peaks all are decreased by irradiation, but the 195 K peak is strongly increased.

To summarize the dielectric results, note that we have observed four relaxation peaks specifically related to the presence of Fe. Two of these at 20 and 138 K, are also related to the presence of Na. It is tempting to regard these peaks as due to Fe-Na pairs, i.e. the analogs of the 30 and 75 K peaks due to the Al-Na center. The ubiquitous 99 K peak is difficult to identify at this stage. Finally, the 195 K peak, which is absent for Na-swept samples and increases upon irradiation, may be considered as possibly due to Fe compensated by H^+, since hydrogen is present both in unswept and H-swept samples.[17] Further, as in the case of Al-related centers in quartz,[18] room-temperature irradiation should liberate the alkali from substitutional Fe^{3+} and allow a proton to be trapped in its place.

Table 2. Activation Energies and Pre-exponentials of Fe-related Peaks

T (K) for 1 kHz	E (eV)	ν_o (sec^{-1})
20	0.030	1.5×10^{11}
99	0.17	4×10^{12}
138	0.22	5×10^{11}
195	0.37	2×10^{13}

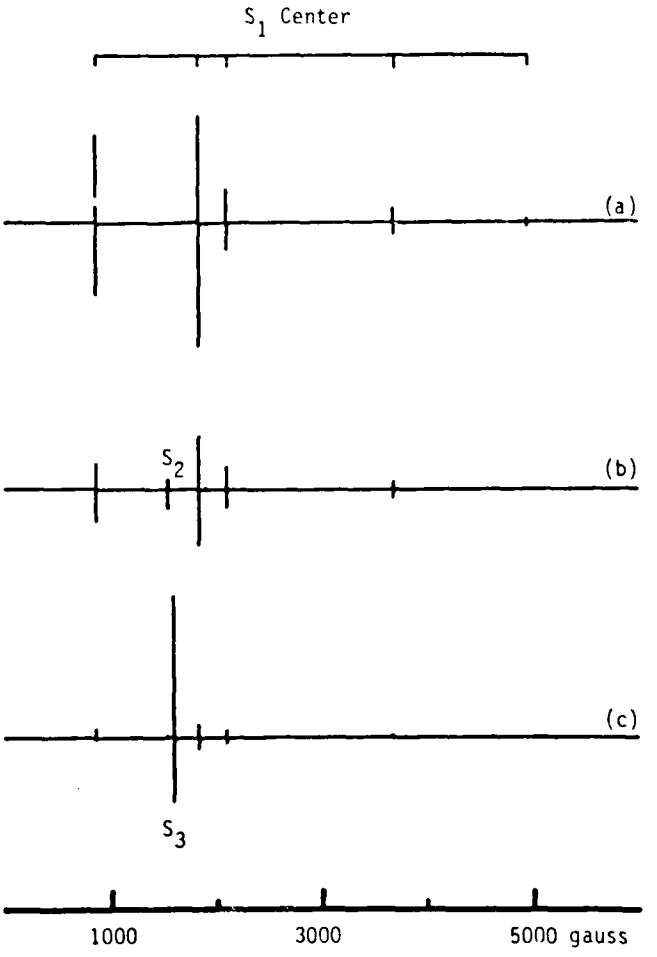

Fig. 4. ESR spectra taken at 27 K with the magnetic field parallel to the c axis. Trace (a) is from the lithium-swept sample, trace (b) is from the hydrogen-swept sample, and trace (c) is from the sodium-swept sample.

Electron Spin Resonance (ESR)

An ESR sample was cut from the center of each of the three samples that had been Li^+, Na^+ and H^+-swept and first studied by DR measurements. Then, an ESR spectrum was taken at 27 K for each sample. Fig. 4 (a) shows the result obtained from the lithium-swept sample. The only spectrum present is the S_1 center. This correlates with an assignment of the S_1 center to a substitutional Fe^{3+} with an adjacent interstitial Li^+ ion. Other cultured amethyst samples which had not been swept but had been heated to the 400-500°C range exhibited a dominant S_1 ESR spectrum just like the

lithium-swept sample. This strongly suggests that the substitutional Fe^{3+} ions in the usual cultured amethyst are nearly all compensated by Li^{+} ions.

Fig. 4 (b) shows the result obtained from the hydrogen-swept sample. This spectrum contains a small S_1 center and also an S_2 center. Since the S_2 center corresponds to a proton compensating the Fe^{3+}, we would suggest that this sample was only partially swept (i.e., many, but not all, of the interstitial lithium ions adjacent to the Fe^{3+} have been replaced with protons).

Fig. 4 (c) shows the result obtained from the sodium-swept sample. This spectrum contains a very small S_1 center and a much larger spectrum which we have labeled the S_3 center. To our knowledge, the S_3 center has not been previously reported in the literature. We assign the S_3 center to a substitutional Fe^{3+} ion with an adjacent interstitial Na^{+} ion. Thus, we suggest that this sample was reasonably well-swept with the major fraction of the interstitial Li^{+} ions being replaced by Na^{+} ions. (This is supported by the appearance of the large Al-Na extra DR peak at 30 K in the Na-swept sample.) An important feature of the S_3 center is a rapid spin-lattice-relaxation time which broadens its ESR spectrum at higher temperatures. We could not observe the S_3 center above approximately 30 K because of this line broadening, whereas the S_1 and S_2 centers can be observed even at room temperature. This rapid spin-lattice-relaxation time is consistent with the small activation energy for the 20 K dielectric loss peak in Na-swept samples (see Table 2).

A striking change is observed in the ESR spectra when a sample is exposed to ionizing radiation at room temperature. The radiation (several Mrads) destroys S_1 or S_3 centers that are initially present and replaces them with S_2 centers. This is illustrated in Fig. 5 for the lithium-swept sample. This is consistent with the concept, already mentioned, that room-temperature irradiation should remove the alkali ion from an Fe^{3+}, thus allowing a proton to replace it. In addition, Al-h centers also appear after irradiation.

Two of the centers reported earlier, viz. the so-called I center and the center observed by Cox,[13] have not been observed in the present work. A likely explanation is that most previous work on ESR of Fe-containing quartz was carried out on natural crystals, which are probably more complex than the present (cultured) crystals.

Interrelation of DR and ESR Results

The two techniques used in this work measure very different defect properties. To obtain a dielectric relaxation (DR) response requires that the defect possess a net dipole moment and be capable of occupying more than one equivalent orientation. For electron spin resonance (ESR) the defect must possess an unpaired spin, so that the spin states can be split by a magnetic field. The ESR technique is particularly sensitive to ions with a $3d^5$ electronic structure (half-filled 3d shell), such as Fe^{3+}.

The newly observed 20 K and 138 K peaks and the newly observed S_3 center are readily linked together, as being caused by the Fe-Na center with the interstitial Na ion off-axis, similarly to the case of the Al-Na center shown in Fig. 1. This reason that this center is observed for the first time in the present work is probably because Li^{+} is the dominant

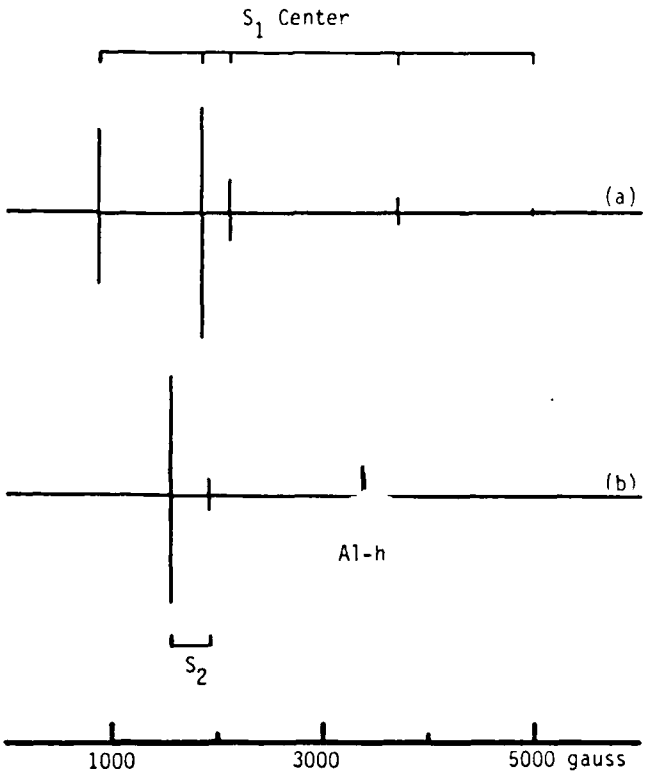

Fig. 5. Effect of room-temperature radiation on the lithium-swept sample. Trace (a) is before irradiation and trace (b) is after irradiation.

alkali in both natural and cultured crystals, so that only after Na-sweeping can Na centers be readily observed. Previous workers did not examine Na-swept Fe-doped quartz.

The S_1 center does not seem to have a DR equivalent. The only possibility is the 99 K peak, but detailed analysis of the spin Hamiltonian for the S_1 spectrum shows that one principal axis is parallel to the 2-fold symmetry axis (or x-axis).[6,7] Since the S_1 center is an Fe-Li pair, this suggests that the Li interstitial resides on the 2-fold axis. But, if this is the case, there is no possibility for the low-temperature reorientation required for DR to take place. The situation for the Fe-alkali pairs then seems to be quite analogous to that for Al-alkali pairs, viz., the Fe-Li lies along the 2-fold axis while Fe-Na is off axis (as in Fig. 1), and therefore, only Fe-Na gives rise to DR. Then to what defect can the ubiquitous 99 K peak be attributed? Since it represents a substantial concentration of Fe and yet is not detected by ESR, it seems reasonable to conclude that it is due to a dipolar defect involving Fe in a valence other than 3+. Further work will be required to establish the nature of this center.

The remaining defects to be discussed are those that produce the S_2 spectrum in ESR and the 195 K peak in DR. It is tempting to regard that these are both the same, namely the Fe-OH defect. The association of the S_2 spectrum with this defect has already been established. In the case of the 195 K peak, the fact that it is present without irradiation (except for the Na-swept sample) and yet increases upon irradiation is strongly suggestive of a proton-related defect. However, the relative intensities of the S_2 spectrum for Na-, Li- and H-swept material both before and after irradiation does not correlate well with the strengths of the 195 K peak. For example, the S_2 has a strong intensity following irradiation of a Na-swept sample, while the 195 K peak is absent for this condition (see the last entry in Table 1). Accordingly, we cannot claim that the simple Fe-OH defect is responsible for the 195 K peak.

In conclusion, the simultaneous use of two major techniques for the study of Fe-related defects in quartz has better enabled us to sort out the wide complexity of defects in such crystals, but further work remains to be done to answer some of the questions raised.

Acknowledgements

The authors are grateful to Dr. B. Sawyer for growing the crystals, to Prof. J.J. Martin for carrying out the sweeping and to R. Hantehzadeh for assistance with the ESR measurements. This work was supported by the U.S. Air Force under contract F-19628-85-C-0104 with Columbia University and contract F-19628-86-C-0138 with Oklahoma State University.

References

1. J.C. King and H.H. Sander, Rad. Effects 26, 203 (1975).
2. L.E. Halliburton, Cryst. Lattice Defects and Amorphous Materials 12, 163 (1985).
3. J. Toulouse and A.S. Nowick, J. Phys. Chem. Solids 46, 1285 (1985).
4. J.J. Martin, J. Appl. Phys. 56, 2536 (1984).
5. J.A. Weil, Phys. Chem. Minerals 10, 149 (1984).
6. D.R. Hutton, Phys. Lett. 12, 310 (1964).
7. T.I. Barry, P. McNamara, and W.J. Moore, J. Chem. Phys. 42, 2599 (1965).
8. G. Lehmann and W. J. Moore, J. Chem. Phys. 44, 1741 (1966).
9. G. Lehmann, Zeits. Naturf. 22a, 2080 (1967).
10. L.M. Matarrese, J.S. Wells, and R.L. Peterson, J.Chem. Phys. 50, 2350 (1969).
11. H.D. Stock and G. Lehmann, J. Phys. Chem. Solids 38, 243 (1977).
12. M.J. Mombourquette, W.C. Tennant, and J.A. Weil, J. Chem. Phys. 85, 68 (1986).
13. R.T. Cox, J. Phys. C: Solid State Phys. 9, 3355 (1976); 10, 4631 (1977).
14. J.C. King, Bell Syst. Tech J. 38, 573 (1959).
15. W.J. De Vos and J. Volger, Physica 47, 13 (1970).
16. J. Toulouse, S. Ling and A.S. Nowick, Phys. Rev., to be published.
17. H.G. Lipson and A. Kahan, J. Appl. Phys. 58, 963 (1985).
18. L.E. Halliburton, N. Koumvakalis, M.E. Markes, and J.J. Martin, J. Appl. Phys. 52, 3565 (1981).

ON THE ROLE OF CRYSTAL DEFECTS AS SOURCES OF RESONATOR FREQUENCY INSTABILITY

Principal Investigator: A. S. Nowick

Henry Krumb School of Mines

Columbia University

New York, N.Y. 10027

Final Technical Report

Period: June 28, 1985 - August 31, 1988

Contract No. F 19628-85-C-0104

Contract Monitor: Mr Herbert G. Lipson

Deputy of Electronic Technology

Hanscom AFB, MA 01731

Sponsored by:

Deputy for Electronic Technology

Rome Air Development Center

Electronic Systems Division

Air Force Systems Command

I. INTRODUCTION

The work under this contract has been concerned with developing an understanding of the crystal defects present in quartz crystals that give rise to frequency instabilities. The work has given rise to four papers that are appended to this report and to material for an additional paper that has yet to be written. Here we will first briefly summarize the contents of the attached papers and, in the next section, will give the principal results of the newest work.

Paper 1, presented at the 40th Annual Frequency Control Symposium deals with the use of low-temperature dielectric relaxation to study the changes that occur during X-ray irradiation and subsequent annealing of Na-swept quartz. Of special importance is the ability to follow changes in the two loss peaks due to Al-Na defects, and the development of an "irradiation peak". Detailed defect models are developed involving Al-Na, Al-hole and Al-OH centers.

Paper 2, presented at a Materials Research Society Symposium, looks at irradiation effects not only on the dielectric loss peaks but also in producing "radiation-induced conductivity", i.e. an enhanced electrical conductivity in the temperature range up to 260°C with an activation energy of 0.29 eV. It appears that the enhanced conductivity is due to electron holes behaving as small polarons.

Paper 3, published in Physical Review, makes a detailed study of the low-temperature dielectric relaxation peak produced upon irradiation of

quartz, and earlier designated as the "irradiation peak". By careful comparison with the EPR spectrum due to the Al-hole center, it was conclusively shown that the irradiation peak is due to the Al-hole center, with tne hole located on the adjacent "long-bond" oxygen atom. This center is further shown to reorient by a one-phonon tunneling process below 6°K and by a multiphonon process above this temperature. The effect of phonon scattering by crystal defects is also demonstrated. It is felt that this paper constitutes an important contribution to the basic physics of the subject.

Paper 4, presented at the 41st Annual Frequency Control Symposium presents our work on Fe-doped quartz. This paper compares the Fe centers seen by EPR measurements (S_1,S_2,S_3 centers) with those Fe centers giving rise to dielectric relaxation peaks (the 20, 99, 138 and 195 K peaks). The 99 and 195 K peaks which are widely present in Fe-doped quartz could not, however, be correlated with any of the EPR centers, and their identity remains obscure.

II. RECENT WORK ON Fe-DOPED QUARTZ

The most recent work on Fe-doped quartz, following that described in Paper 4, is aimed at trying to identify the 99 K and 195 K dielectric peaks. In this work, further collaboration between our laboratory, the group doing EPR measurements at Oklahoma State University, and H.G. Lipson at RADC Hanscom, carrying out measurements of IR absorption, were involved.

In order to better identify the Fe-containing centers that are present, we have carried out a series of gamma-ray irradiations and anneals on the Fe-doped samples. The work on dielectric relaxation and EPR were carried out on identically treated adjacent samples, while the IR was on a similar sample identically irradiated and annealed. Figure 1 shows the results of irradiation for the various centers on a plot in which the intensities measured (heights of dielectric peak or intensity of EPR spectrum) are all normalized to unity. Shown are the 99 K and 195 K dielectric peaks and the S1 and S2 EPR spectra, as well as the Al-hole EPR spectrum. Note that Al-hole, S2 and 195 K peak all increase with irradiation while the S1 and 99 K peak decrease.

Figure 2 shows the results of 1/2 hour annealing at various temperatures, again using normalized intensities. Clearly, all centers that increased upon irradiation decrease upon annealing and vice versa.

The S1 center is believed to be due to Fe-Li, while the S2 is due to Fe-OH. On the other hand, the dielectric peaks do not correlate with these

EPR centers. Thus, from Fig.1, the S2 and 195 K do not behave similarly to each other. From Fig.2, the S1 and 99 K also clearly cannot be regarded as identical centers.

This work is yet to be completed with inclusion of the IR measurements. Upon completion, it is expected that we will submit a joint paper on this study of Fe-doped quartz to the Journal of Applied Physics.

Fig. 1 Effect of Cs137 irrad. on EPR and DR

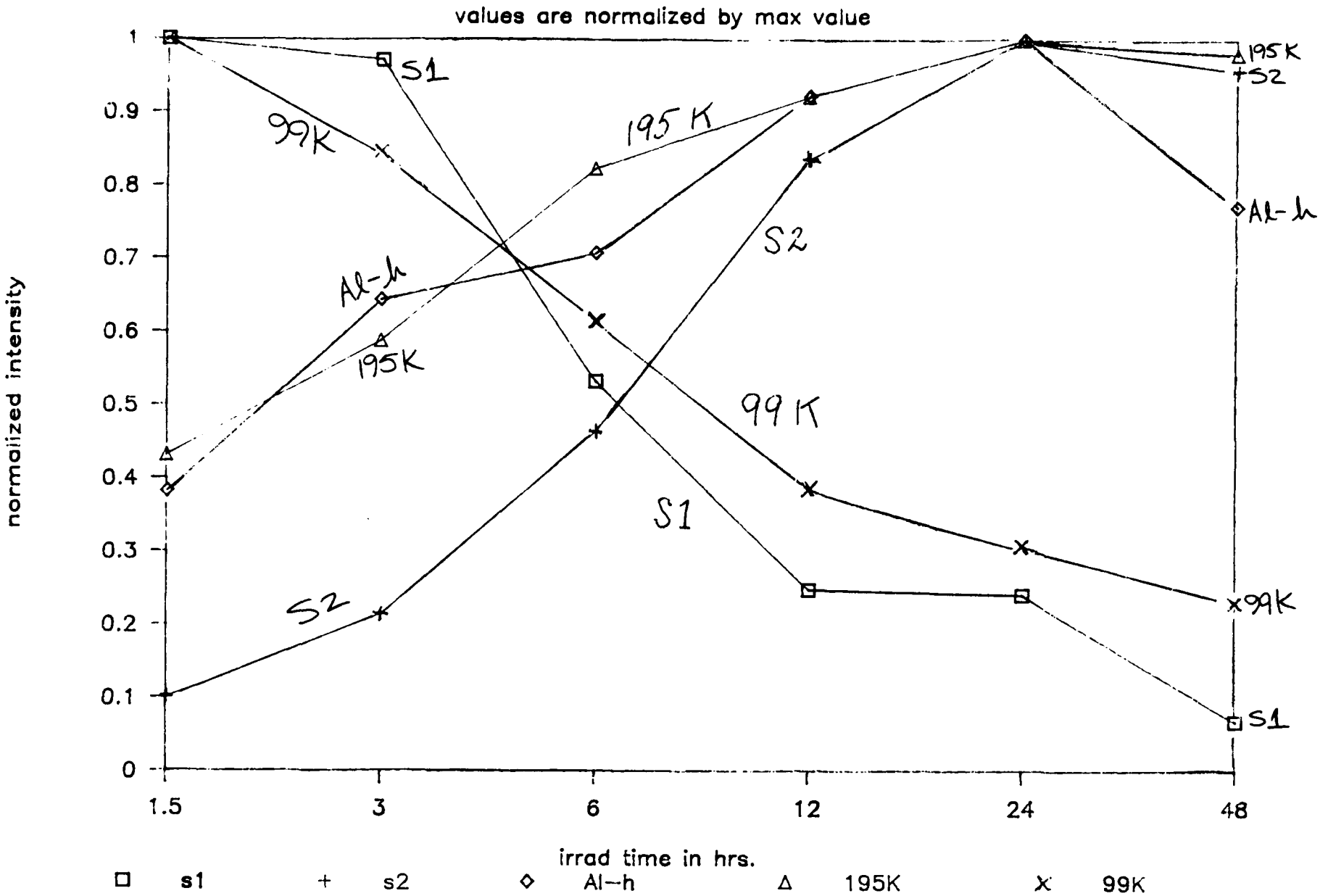

Fig. 2 Effect of 1/2hr anneal after 24hr irrad

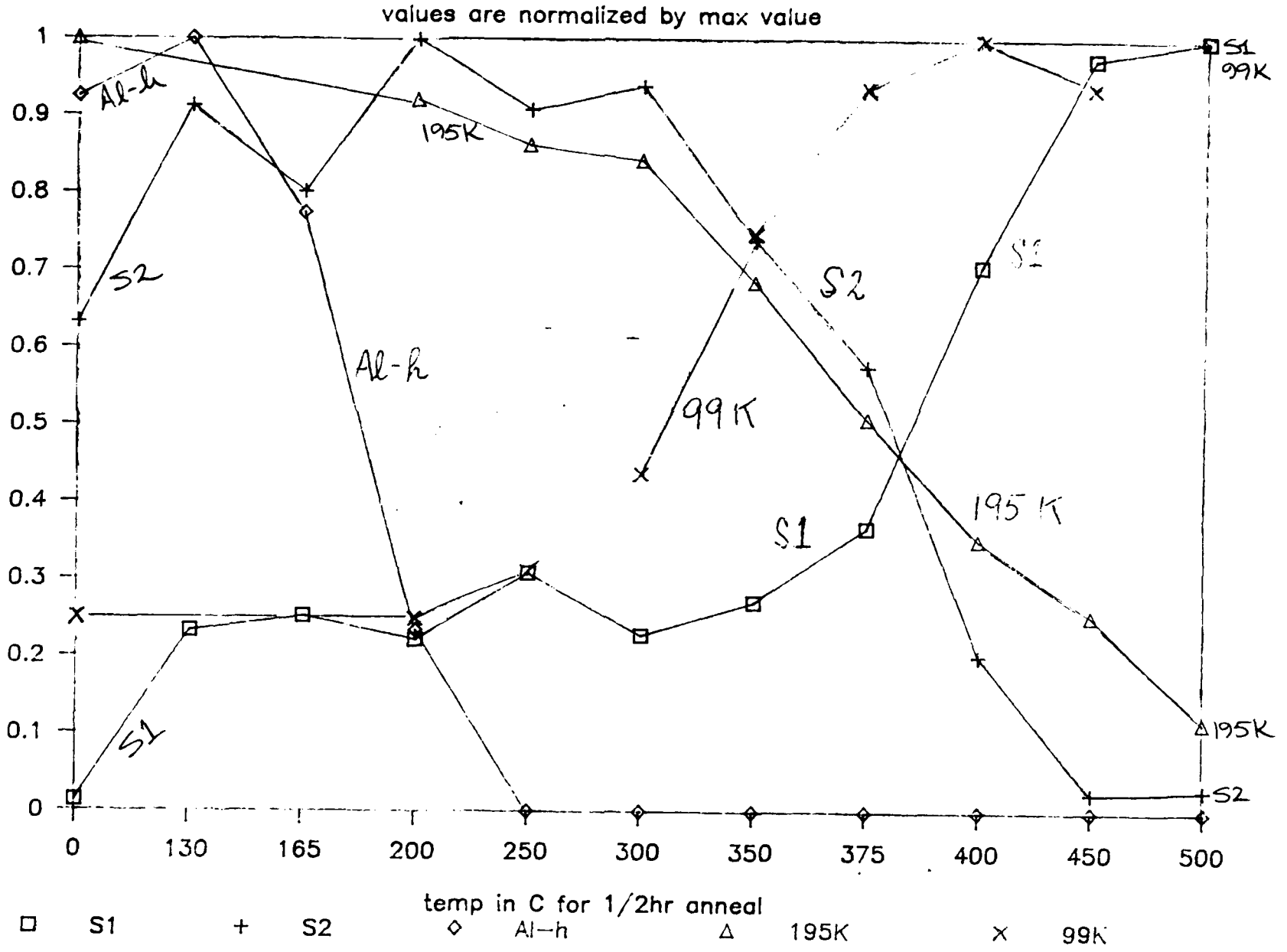

REFERENCES

1. S. Ling and A.S. Nowick, "Study of Irradiation Effects in Quartz Crystals Using Low-temperature Dielectric Relaxation", Proc. 40th Annual Frequency Control Symp., IEEE, p.96 (1986).

2. S. Ling, B.S. Lim and A.S. Nowick, "Effect of Irradiation on the Electrical Properties of α-Quartz Crystals", Materials Research Soc. Symp., Vol. 60, p.443 (1986).

3. J. Toulouse, S. Ling and A.S. Nowick, "Dielectric Relaxation of the Aluminum-hole Center in α-Quartz: An Example of Phonon-Assisted Tunneling", Physical Review B37, 7070 (1988).

4 S. Keilson, S. Ling and A.S. Nowick, "Dielectric Relaxation and EPR in Quartz Crystals Containing Fe", Proc. 41st Annual Frequency Control Symp., IEEE, p.223 (1987).